# Flow energy harvesting with piezoelectric plates

Olivier Doaré
IMSIA, ENSTA Paristech

LMT
9 mars 2017

Sébastien Michelin, LadHyX
Miguel Pineirua, IMSIA
Yifan Xia, IMSIA, LadHyX

# La piézoélectricité

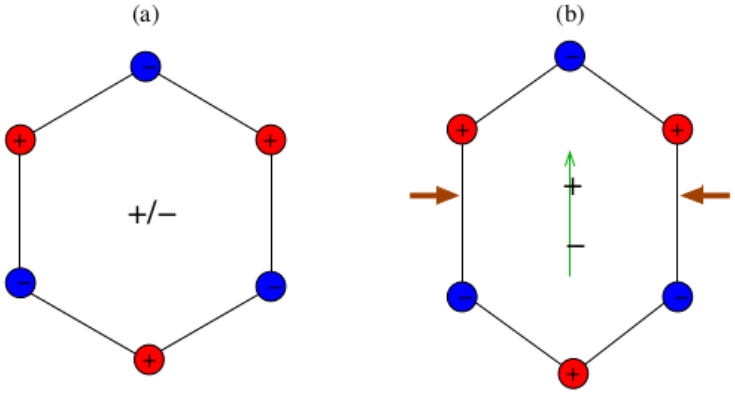


Déplacement du barycentre des charges positives et négatives

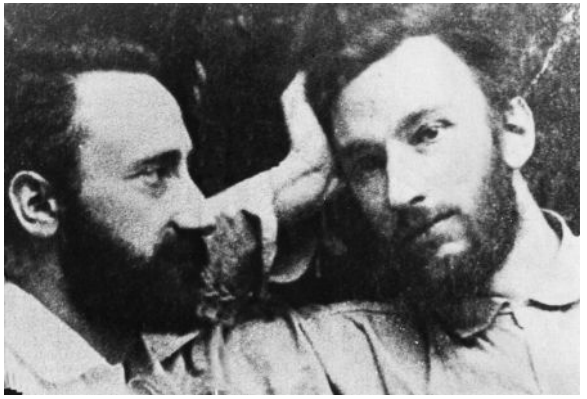

Jacques Curie

Pierre Curie

Gabriel Lippman

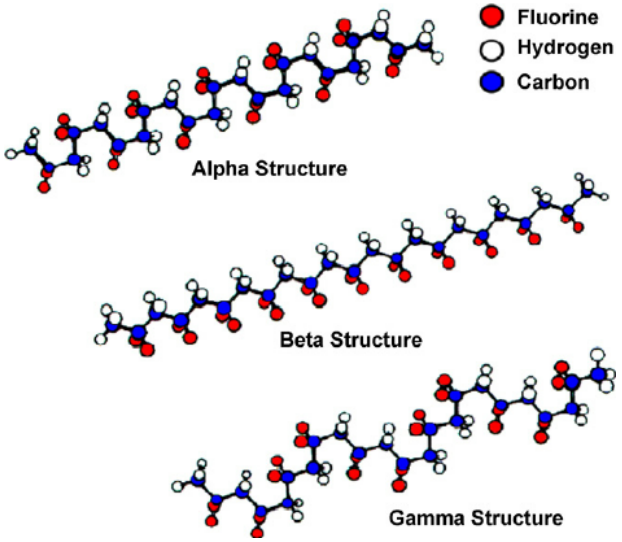


**Polyfluorure de vinylidène**

**(PVDF)**

# Modélisation 3D

- Milieu élastique linéaire
- Les champs de contrainte mécanique et électrique sont couplés linéairement
- Le matériau piézoélectrique est un diélectrique

| Comportement | Équilibre |
| --- | --- |
| $\underline{\underline{\sigma}} = \underline{\underline{\underline{C}}} : \underline{\underline{\varepsilon}} - \underline{\underline{e}}^{\mathrm{t}}.\underline{E}$ | $\rho_s \dfrac{\partial^2 \underline{\xi}}{\partial t^2} = \mathrm{div}\underline{\underline{\sigma}}$ |
| $\underline{D} = \underline{\underline{e}} : \underline{\underline{\varepsilon}} + \underline{\underline{d}}.\underline{E}$ | $\mathrm{div}\underline{D} = 0$ |

$\rho_s$ Masse volumique

$\underline{\underline{\sigma}}$ Tenseur des contraintes

$\underline{\xi}$ Champ de déplacement

$\underline{\underline{\varepsilon}}$ Tenseur de déformation

$\underline{E}$ Champ électrique

$\underline{D}$ Champ de déplacement électrique

$\underline{\underline{\underline{C}}}, \underline{\underline{e}}, \underline{\underline{d}}$ Tenseurs d'élasticité, de couplage piézoélectrique, de permitivité électrique

# Film mince, ajout d'électrodes

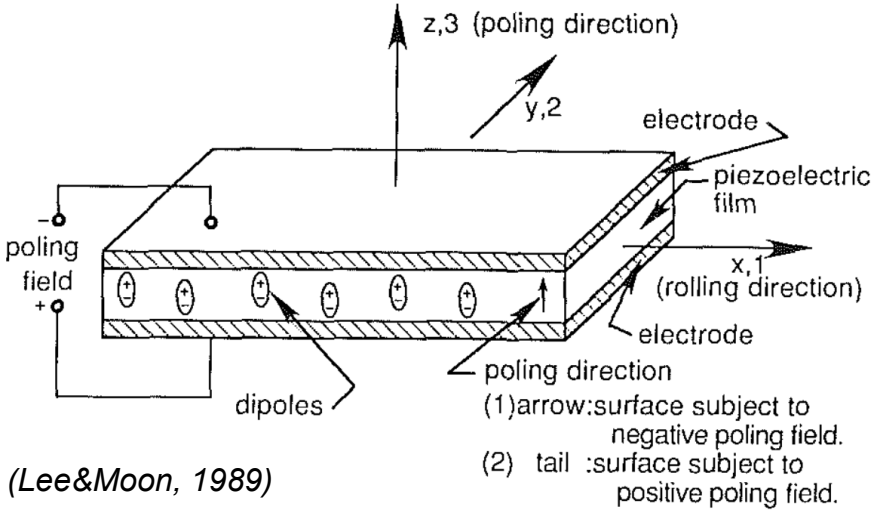


*(Lee&Moon, 1989)*

- Milieu orthotrope, isotrope plan
- Film piézo électrodes sur les faces supérieures et inférieures → champ électrique dans la direction z

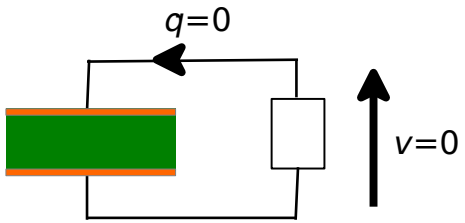


Milieu non déformé, à l'équilibre ↔ tension/courant nuls

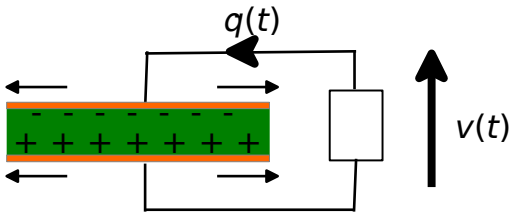


Milieu déformé ↔ tension/courant

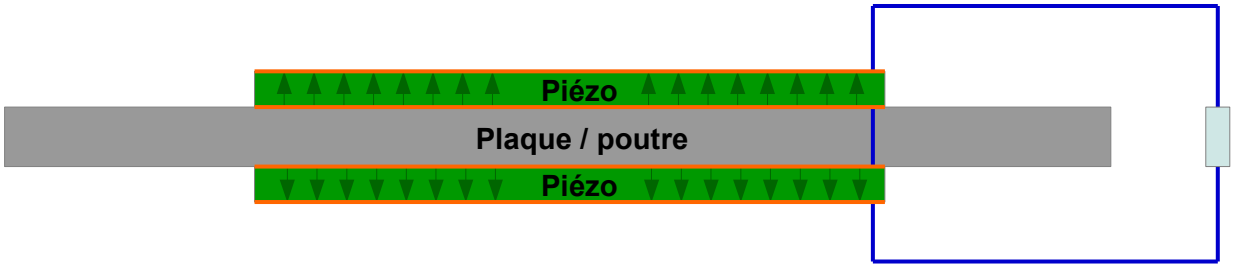


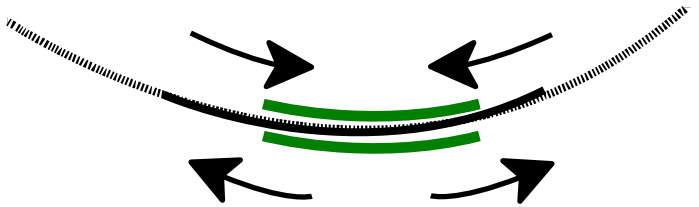

Couplage entre champ électrique et déformation de flexion

# Plaque + 2 patchs piézoélectriques

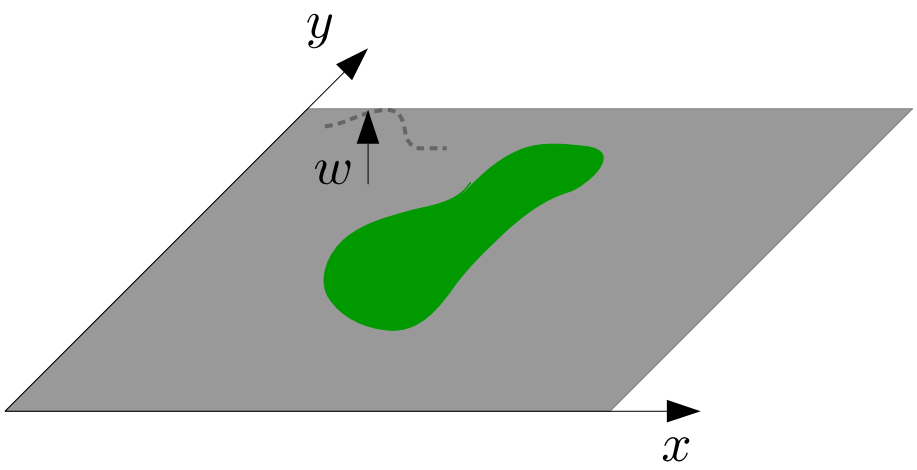


| | |
|---|---|
| $F_p$ | Fonction de polarisation |
| $D$ | Rigidité de flexion |
| $\mu$ | Masse surfacique |
| $Q$ | Déplacement de charges |
| $Z_p$ | Bras de levier |
| $C$ | Capacité de la paire de piézo |
| $w(x,y,t)$ | Déplacement |

Le système couplé dans le cas d'une plaque de Kirshoff-Love s'écrit :

$$D\Delta^2 w + \mu\ddot{w} = -2U Z_p h_p \left( e_{31}\frac{\partial^2 F_p}{\partial x^2} + e_{32}\frac{\partial^2 F_p}{\partial y^2} + e_{36}\frac{\partial^2 F_p}{\partial y \partial x} \right)$$

$$\frac{Q}{C} + Z_p \int_S F_p \left( e_{31}\frac{\partial^2 w}{\partial x^2} + e_{32}\frac{\partial^2 w}{\partial y^2} + e_{36}\frac{\partial^2 w}{\partial y \partial x} \right) \mathrm{d}S = U$$

(Lee & Moon, 1989, 1990)

# Cas étudiés : milieux axi ou 1D

Contrôle des modes vibratoires d'un haut-parleur plan

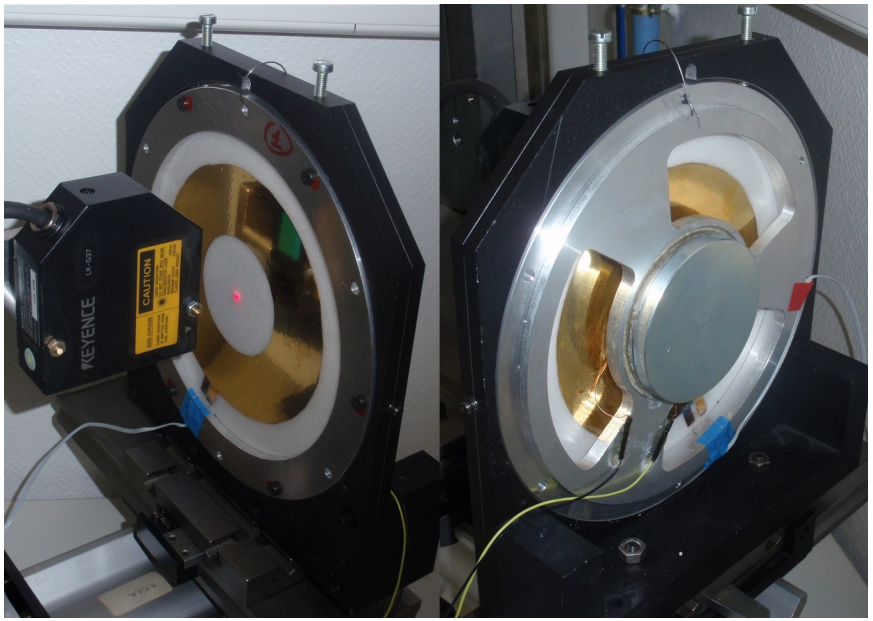


*(OD et al, Journal of Vibration and Acoustics, 2013)*

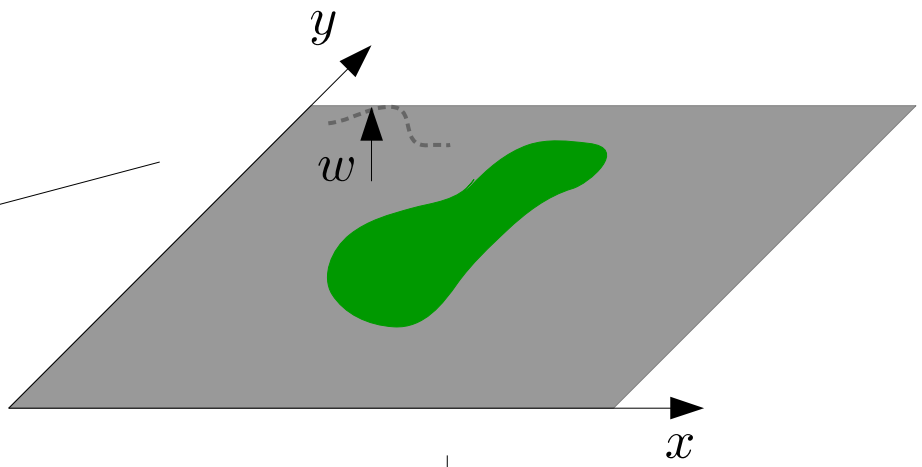


Récupération d'énergie du flottement de plaques minces sous écoulement

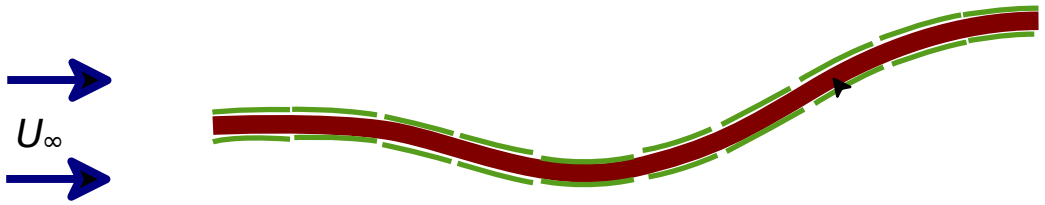

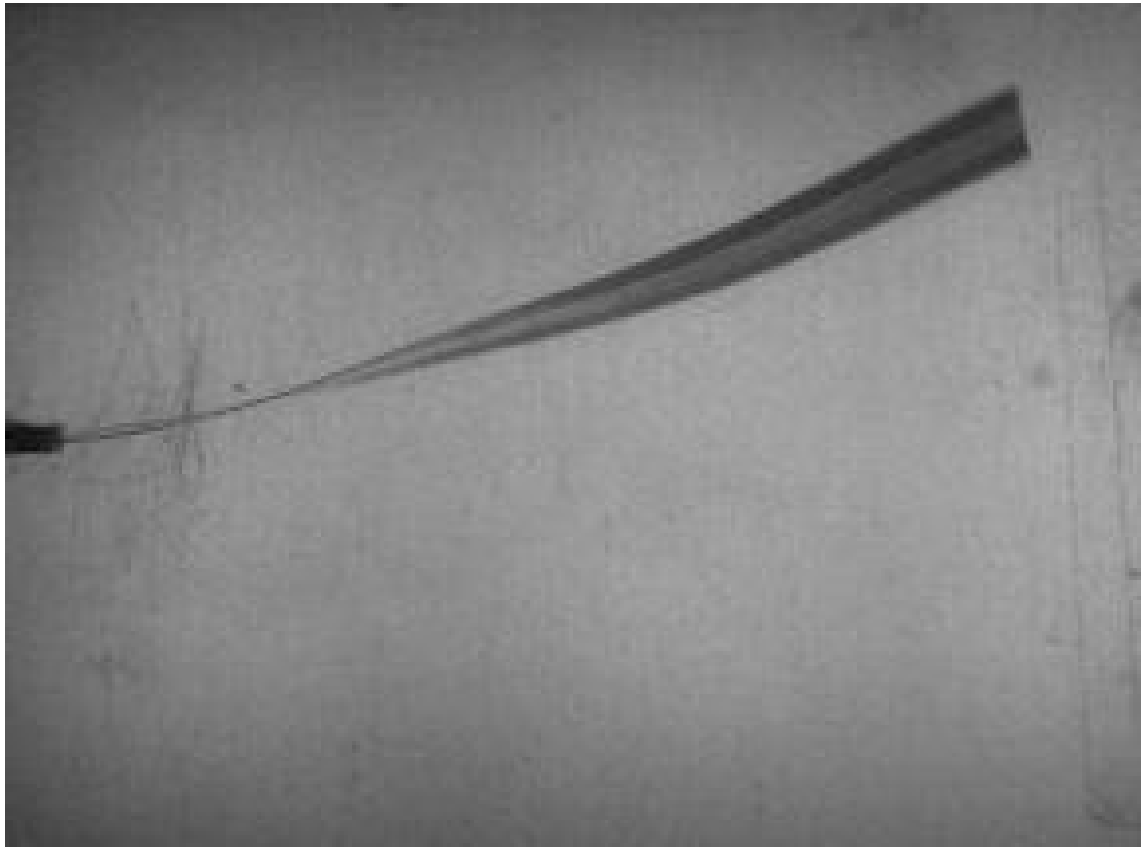

# OUTLINE

**Flow energy harvesting with piezoelectric plates**

Flow energy harvesting

The piezoelectric flag

Linear stability and efficiency

Non linear vibrations and efficiency

Coupling with resonant circuits

Discrete distributions of electrodes

Conclusions

# OUTLINE

**Flow energy harvesting with piezoelectric plates**

Flow energy harvesting

The piezoelectric flag

Linear stability and efficiency

Non linear vibrations and efficiency

Coupling with resonant circuits

Discrete distributions of electrodes

Conclusions

# Energy harvesting from flow-induced vibrations

## Flapping wings

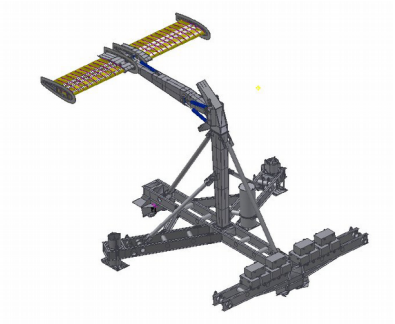

© 2003 - The Engineering Business Ltd

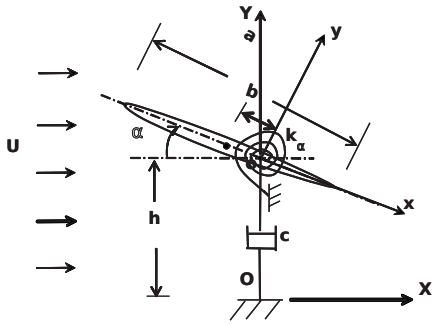


Peng & Zhu, Phys. Fluids, 2009

## Vortex Induced Vibrations (VIV)

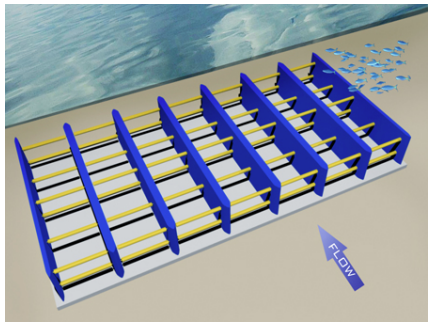


©2011 Vortex Hydro Energy

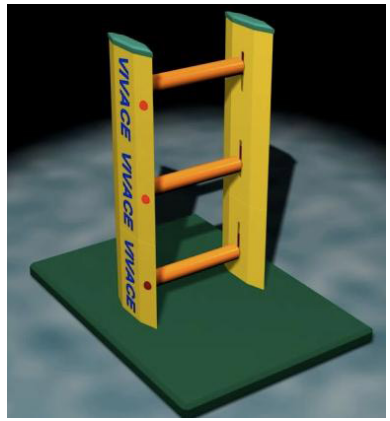


## Vibrations of slender structures in instationnary flows

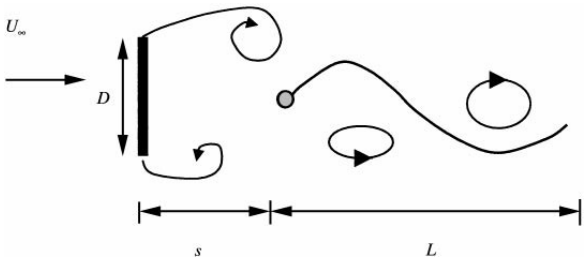


Alen & Smnith, JFS 2002

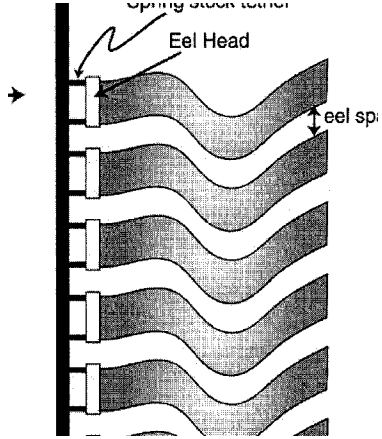


Techet et al., ISOPE 2002

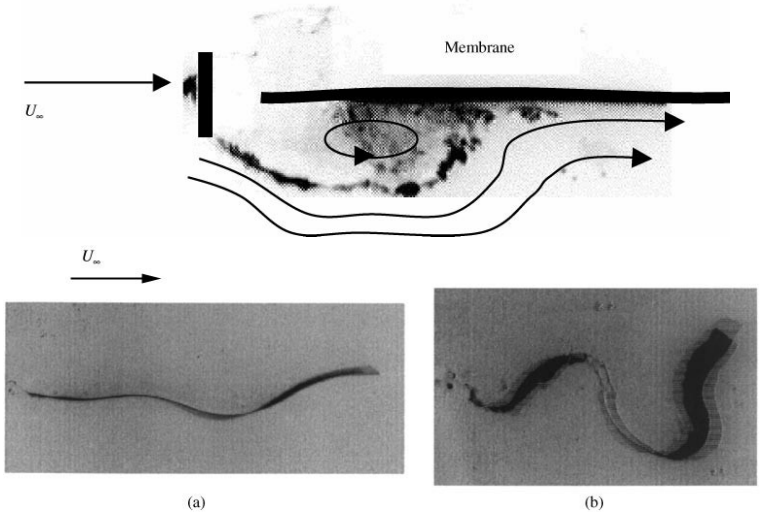


Alen & Smith, JFS 2002

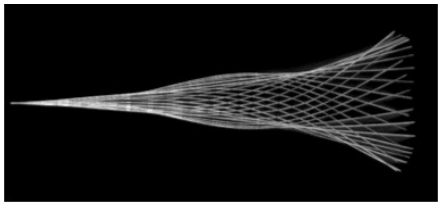

Flapping plate in wind-tunnel
Eloy *et al.*, *J. Fluid Mech.*, 2008

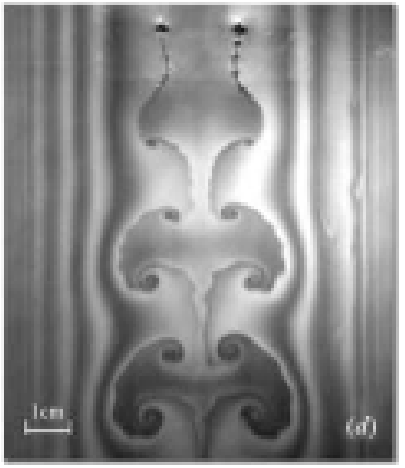

Flapping filaments in soap film flows
Jia *et al.*, *J. Fluid Mech*., 2007

**Instability mechanism :**

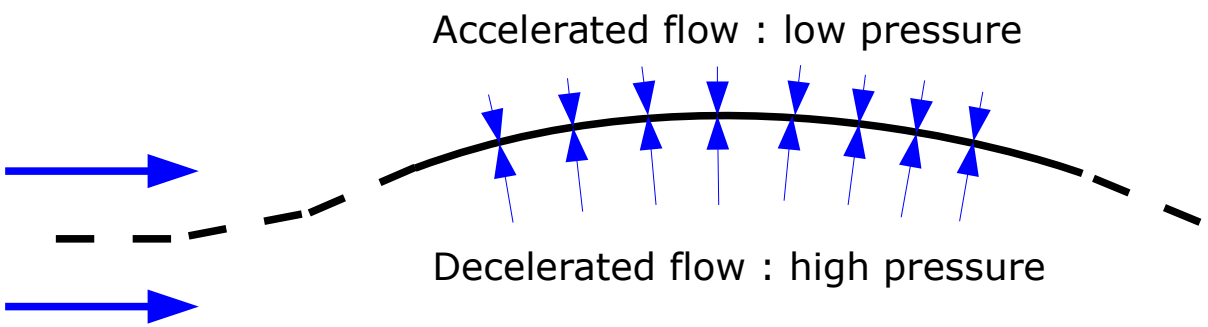


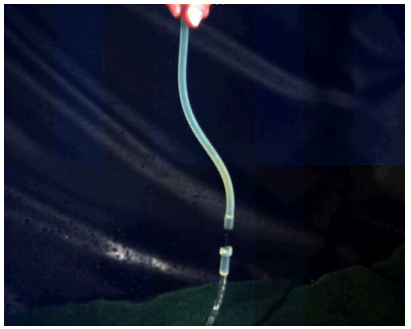

Fluid-conveying pipe

Pressure : destabilizing, scales as $U^2$

Elasticity : stabilizing, constant

→ Instability at a critical velocity

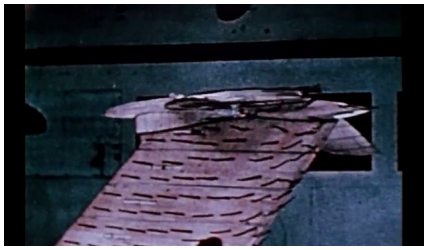

Wing profile

# OUTLINE

**Flow energy harvesting with piezoelectric plates**

Flow energy harvesting

The piezoelectric flag

Linear stability and efficiency

Non linear vibrations and efficiency

Coupling with resonant circuits

Discrete distributions of electrodes

Conclusions

# Energy harvesting from flutter of piezoelectric plates

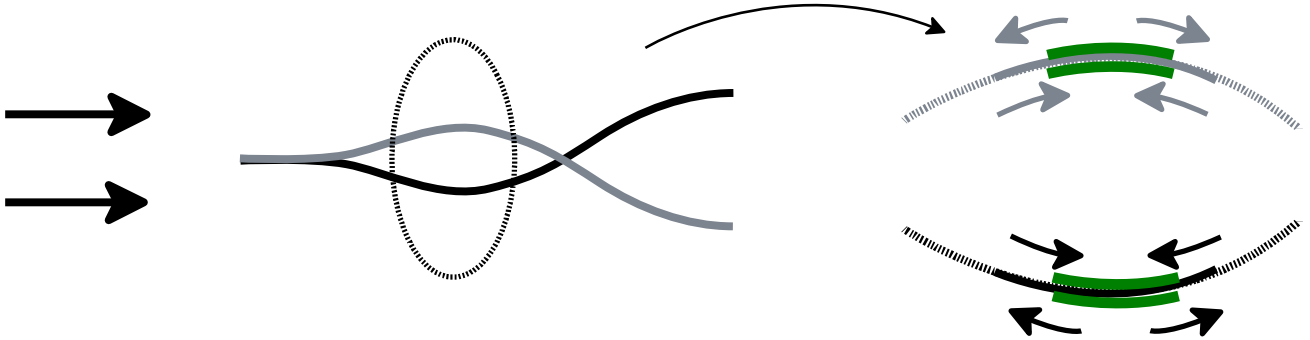

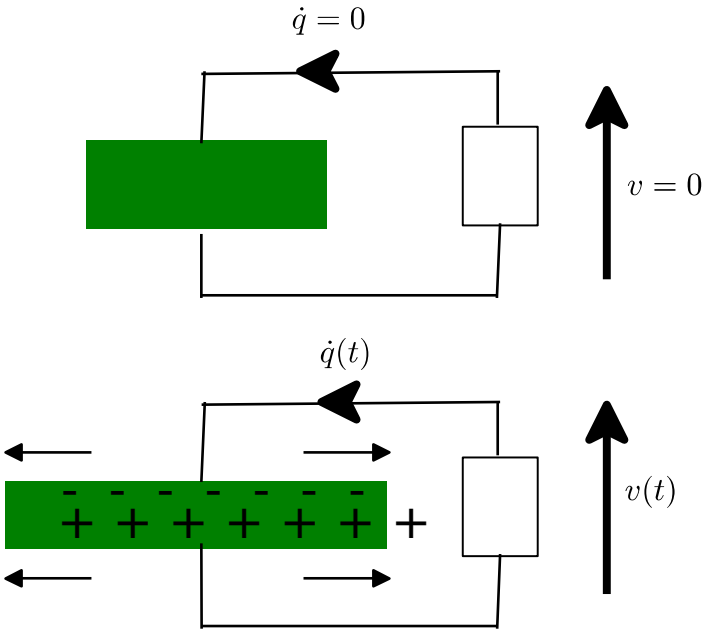


- Defomation → charge transfer between electrodes

$$Q = CV + \chi \int_{s^-}^{s^+} F_p(s)\theta'(s)ds \quad = CV + \chi[\theta]_{s^-}^{s^+}$$

- Voltage → Momentum exerted on the plate

$$\mathcal{M}_{piezo}(s) = -\chi V F_p(s) = -CV[H(s-s^-) - H(s-s^+)]$$

- Shape function of the piezo

$$F_p(s) = H(s-s^-) - H(s-s^+)$$

- **Objective :** Quantify theoretically the maximum efficiency of the system
- The full fluid-solid-electric coupling needs to be taken into account : **NEW**
- **Present approach :** harvested energy modeled by the energy dissipated in a shunted resistance

# Coupled fluid-solid-electric wave equations

Plate with piezoelectric patches shunted by resistive elements

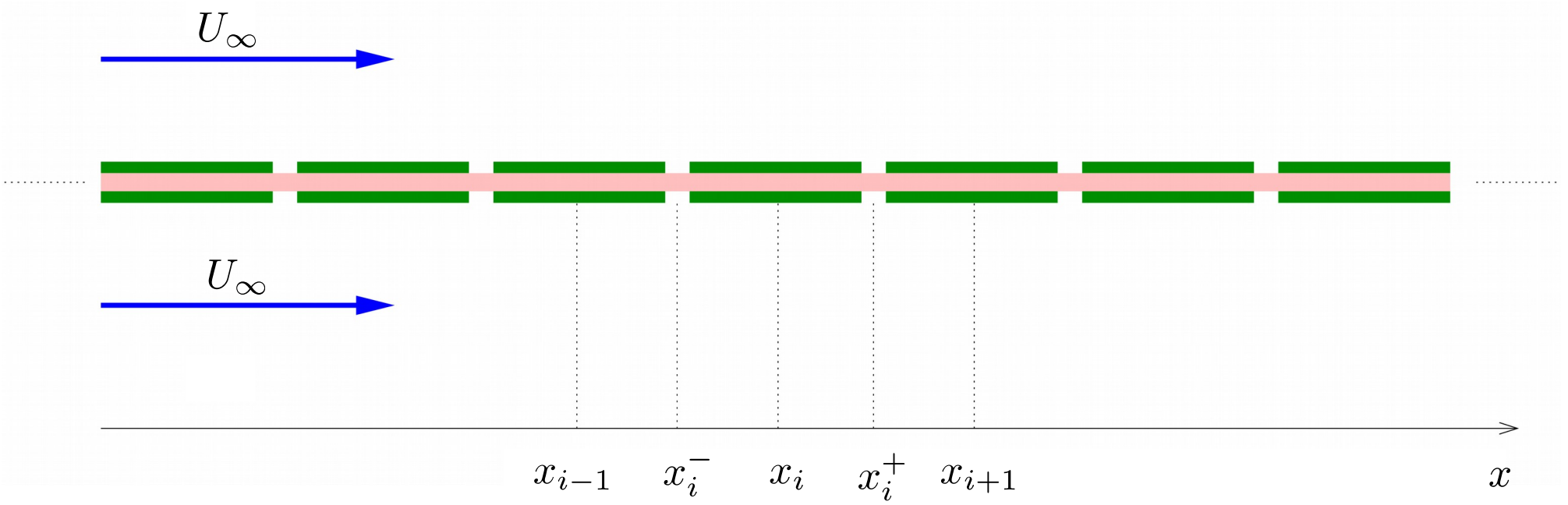


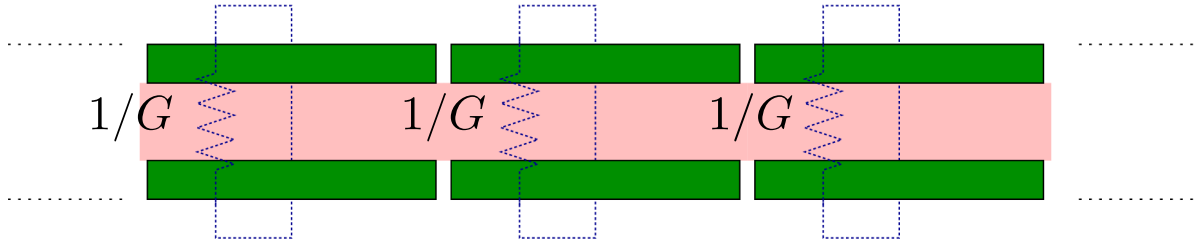


Ohm's law :

$$\frac{\dot{Q}_i}{G} + V_i = 0$$

# Long waves limit → Continuous distribution of piezoelectric patches

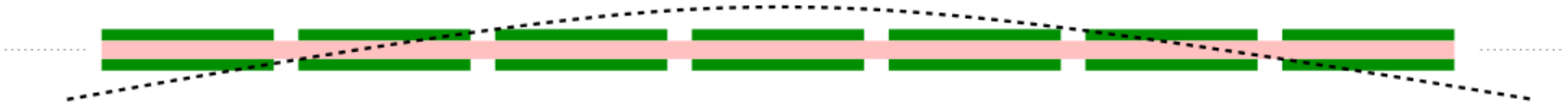

$$\left[\theta\right]_{s^-}^{s^+} \simeq \theta'(s_i)l \qquad \sum_i \bar{V}_i[H(s-s^-) - H(s-s^+)] \simeq v(s)$$

# OUTLINE

**Flow energy harvesting with piezoelectric plates**

Flow energy harvesting

The piezoelectric flag

Linear stability and efficiency

Non linear vibrations and efficiency

Coupling with resonant circuits

Discrete distributions of electrodes

Conclusions

# Linear model

- Infinite span elastic plate with efforts coming from the flow :

$$\mu \ddot{w} = -\mathcal{M} - [P]$$

- Piezoelectric couplings :

Direct : $Q_i = CV_i + \chi[w']_{x_i^-}^{x_i^+}$

Inverse : $\mathcal{M} = -Bw'' - CV_i[H(x - x_i^-) - H(x - x_i^+)]$

- Resistive electrical circuits : $\frac{\dot{Q}_i}{G} + V_i = 0$

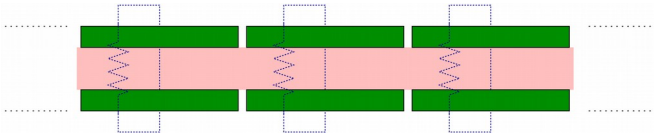

- Long wave limit : $\left[w'\right]_{x_i^-}^{x_i^+} \simeq w''(x_i)l \quad \sum_i \bar{V}_i[H(x - x_i^-) - H(x - x_i^-)] \simeq v(x)$

$$q(x_i) = \frac{Q_i}{l}$$

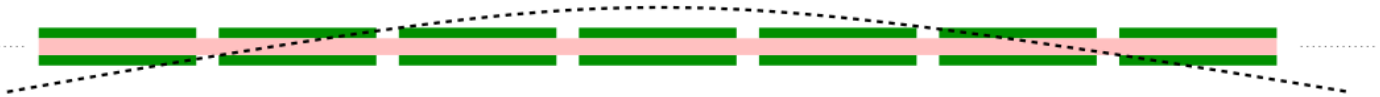

$$c = \frac{C}{l}$$

$$g = \frac{G}{l}$$

# Final model in the form of coupled wave equations

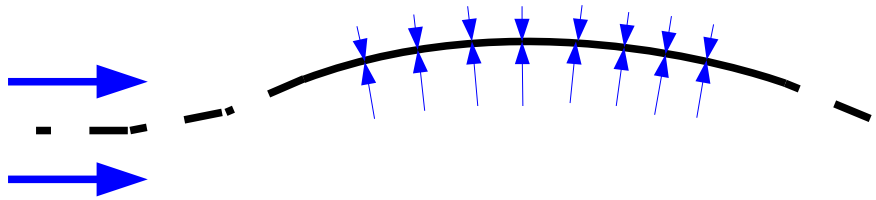

Euler-Bernoulli beam

Pressure jump

$$\left(B + \frac{\chi^2}{c}\right) w'''' + \mu\ddot{w} - \frac{\chi}{c} q'' = -[P]$$

$$\frac{c}{g}\dot{q} + q - \chi w'' = 0$$

Added rigidity due to electrical energy stored in the capacities

Piezoelectric coupling

Capacity discharging in a resistance

# Linear efficiency

- Linear efficiency :

$$\eta_l = \frac{\text{Energy harvested in the electrial circuits during one period}}{\text{Mean of the energy in the system during one period}} \propto \frac{A^2}{A^2}$$

=> Bounded in the linear case

$$r_l = \frac{\int_0^T \langle P_{el} \rangle dt}{\frac{1}{T}\int_0^T \langle E \rangle dt} \quad \text{with } P_{el} = -v\dot{q}, \quad E = \frac{1}{2}\rho_s \dot{w}^2 + \frac{1}{2}B{w''}^2 + \frac{1}{2}cv^2$$

- Which unstable wave or mode maximizes this efficiency ?

$\langle . \rangle \equiv$ Spatial average (on a wave or an eigenmode)

# Linear stablity analysis in the infinite medium (wave analysis)

$$\frac{1}{V^{*2}}(1+\alpha^2)w'''' + \ddot{w} - \frac{\alpha}{V^*}q'' = -[p]$$

$$\gamma\dot{q} + q - \frac{\alpha}{V^*}w'' = 0$$

$$V^* = \sqrt{\frac{\mu^3 U_\infty^2}{B\rho_f^2}} \text{ (Non dimensional velocity)}$$

$$\alpha = \frac{\chi}{\sqrt{cB}} \text{ (Coupling coefficient)}$$

$$\gamma = \frac{\rho_f U_\infty c}{\mu g} \text{ (Timescales ratio)}$$

# Pressure calculation → Dispersion relation

- Perturbation in the form of a wave transporting mechanical and charge displacements :

$$\begin{pmatrix} w \\ q \end{pmatrix} = \left[ \begin{pmatrix} w_0 \\ q_0 \end{pmatrix} e^{i(kx-\omega t)} \right]$$

- Pressure calculated using inviscid, irrotational flow model :

$$[p] = p(x, y = 0^+, t) - p(x, y = 0^-, t) = \left[ 2w_0 \frac{(\omega - k)^2}{|k|} e^{i(kx-\omega t)} \right]$$

- Dispersion relation :

$$\mathcal{L}(V^*, \alpha, \gamma, k, \omega) \begin{pmatrix} w_0 \\ q_0 \end{pmatrix} = \begin{pmatrix} 0 \\ 0 \end{pmatrix} \quad \Rightarrow \quad \boxed{\mathrm{Det}(\mathcal{L}) = 0} \Rightarrow \; D(k, \omega) = 0$$

- Stability condition :

$$\forall k \in \mathtt{R}, \mathrm{Im}(\omega) \leq 0 \Rightarrow \quad \mathrm{Stable}$$

# Stability analysis / effect of energy harvesting

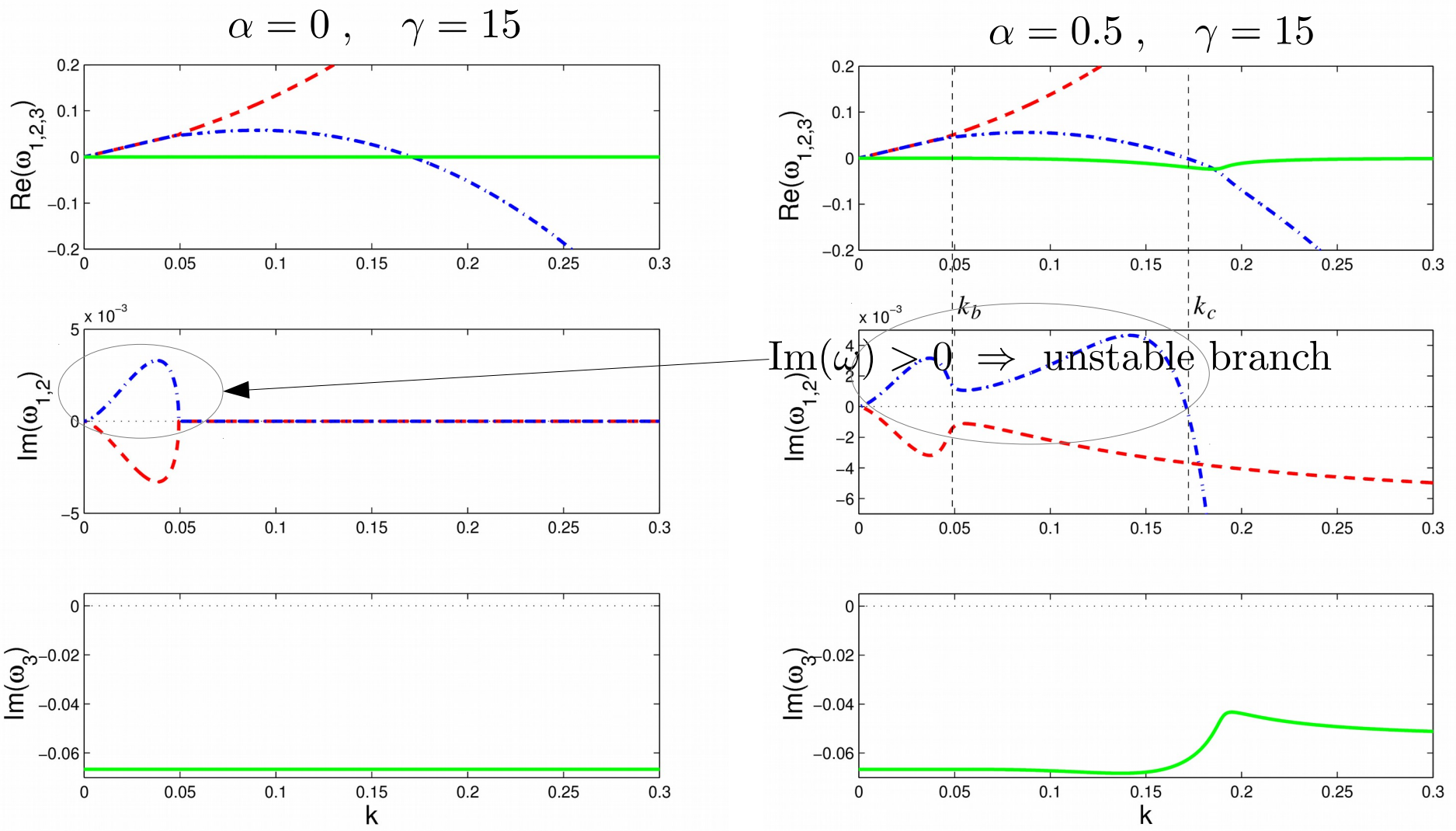


Piezoelectric coupling destabilizes the medium, due to negative energy waves.
(see von Laue 1905, Cairns 1979)

# Wave energy and effect of viscous damping

- Dispersion relation without damping :

$$D(k,\omega) = 0$$

- Dispersion relation with a small amount of viscous damping :

$$D_c(k,\omega+\delta\omega) = D(k,\omega+\delta\omega) - ic(\omega+\delta\omega) = 0$$

- At first order, the perturbation of the frequency satisfies :

$$\delta\omega \left.\frac{\partial D}{\partial \omega}\right|_{(k,\omega)} - ic\omega = 0$$

- Perturbation of the growth rate :

$$\delta\sigma = \frac{c\omega}{\partial D/\partial\omega}$$

- In the context of the dynamics of the interface between two non-miscible fluids, Cairns introduced the wave energy as the work done to generate the wave from $t = -\infty$ to $0$:

$$E = -\frac{\omega}{4}\frac{\partial D}{\partial \omega} y_0^2$$

- $\delta\sigma$ has the opposite sign of the wave energy

# Local stability analysis / effect of energy harvesting

- Piezoelectric coupling : same behaviour, destabilization of a negative energy waves range.
- Perturbation of the growth rate :

$$\delta\sigma \simeq \frac{\omega\alpha^2\gamma k^4}{V^2(1+\omega^2\gamma^2)\dfrac{\partial D}{\partial\omega}}$$

$$V = \sqrt{\frac{\mu^3 U_\infty^2}{B\rho_f^2}} \text{ (Non dimensional velocity)}$$

$$\alpha = \frac{\chi}{\sqrt{cB}} \text{ (Coupling coefficient)}$$

$$\gamma = \frac{\rho_f U_\infty c}{\mu g} \text{ (Timescales ratio)}$$

$\rightarrow$ destabilization

# Which wave and what values of the parameters maximize efficiency ?

1. For a given unstable wave : $\gamma_{opt} \sim 1/\mathrm{Re}(\omega)$

2. Wavenumber that maximize efficiency

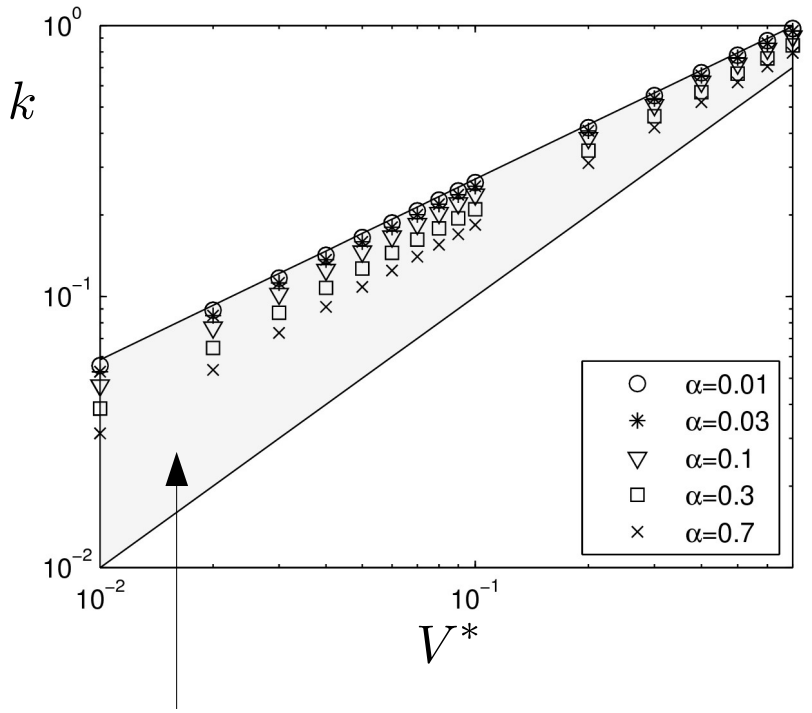


Range of negative energy waves

3. Influence of the coupling coefficient

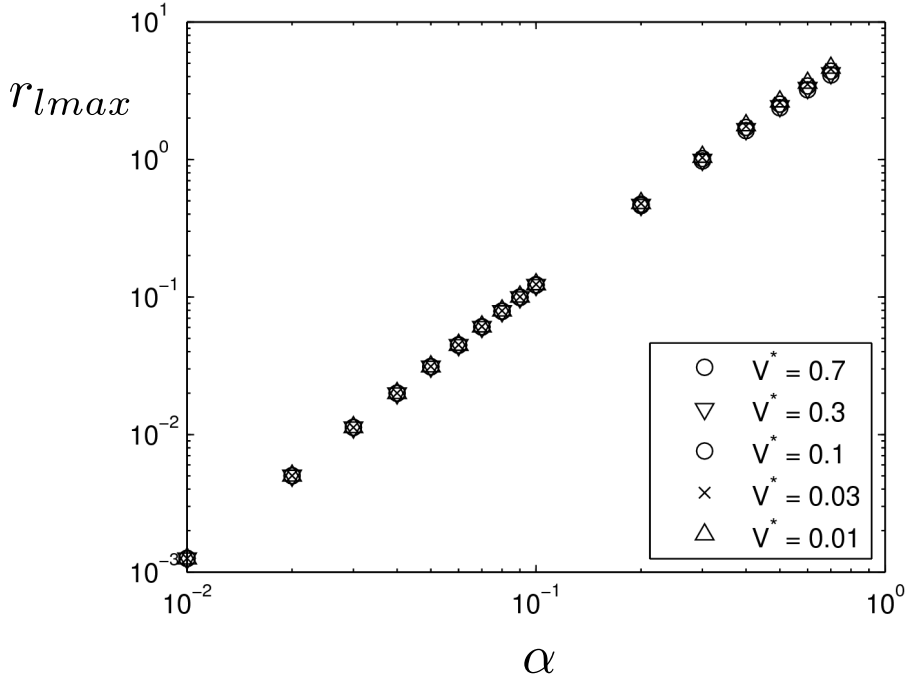


Maximum efficiency scales as $\alpha^2$

# Finite length system

Dimensionless equation, parameters and boundary conditions :

$$\frac{1}{U^{*2}}(1+\alpha^2)w'''' + \ddot{w} - \frac{\alpha}{U^*}q'' = -M^*[p]$$

$$\beta\dot{q} + q - \frac{\alpha}{U^*}w'' = 0$$

$$M^* = \frac{\rho_f L}{\mu}, \quad U^* = UL\sqrt{\frac{\mu}{B}} = V^*M^*, \quad \beta = \frac{cU_\infty}{gL} = \frac{\gamma}{M^*}, \quad \alpha = \frac{\chi}{\sqrt{cB}}.$$

$$\text{for } x=0 \quad \begin{cases} w = 0 \\ w' = 0 \end{cases} \quad \text{for } x=1 \quad \begin{cases} (1+\alpha^2)w'' - \alpha U^* q = 0 \\ (1+\alpha^2)w''' - \alpha U^* q' = 0 \end{cases}.$$

Solution sought in the form of global modes :

$$\begin{pmatrix} w \\ q \end{pmatrix} = \begin{pmatrix} W(x) \\ Q(x) \end{pmatrix} e^{-\mathrm{i}\omega t}$$

Linear expression of the pressure as function of the displacement W(x)
Discretization → Eigenvalue problem → Discrete set of eigenfrequencies
Instability if $\exists\, \omega_j \ \setminus \ \mathrm{Im}(\omega_j) > 0$

# Global analysis :Conversion efficiency of the dominant unstable mode

$$\alpha = 0.5 \quad \beta = 0.25$$

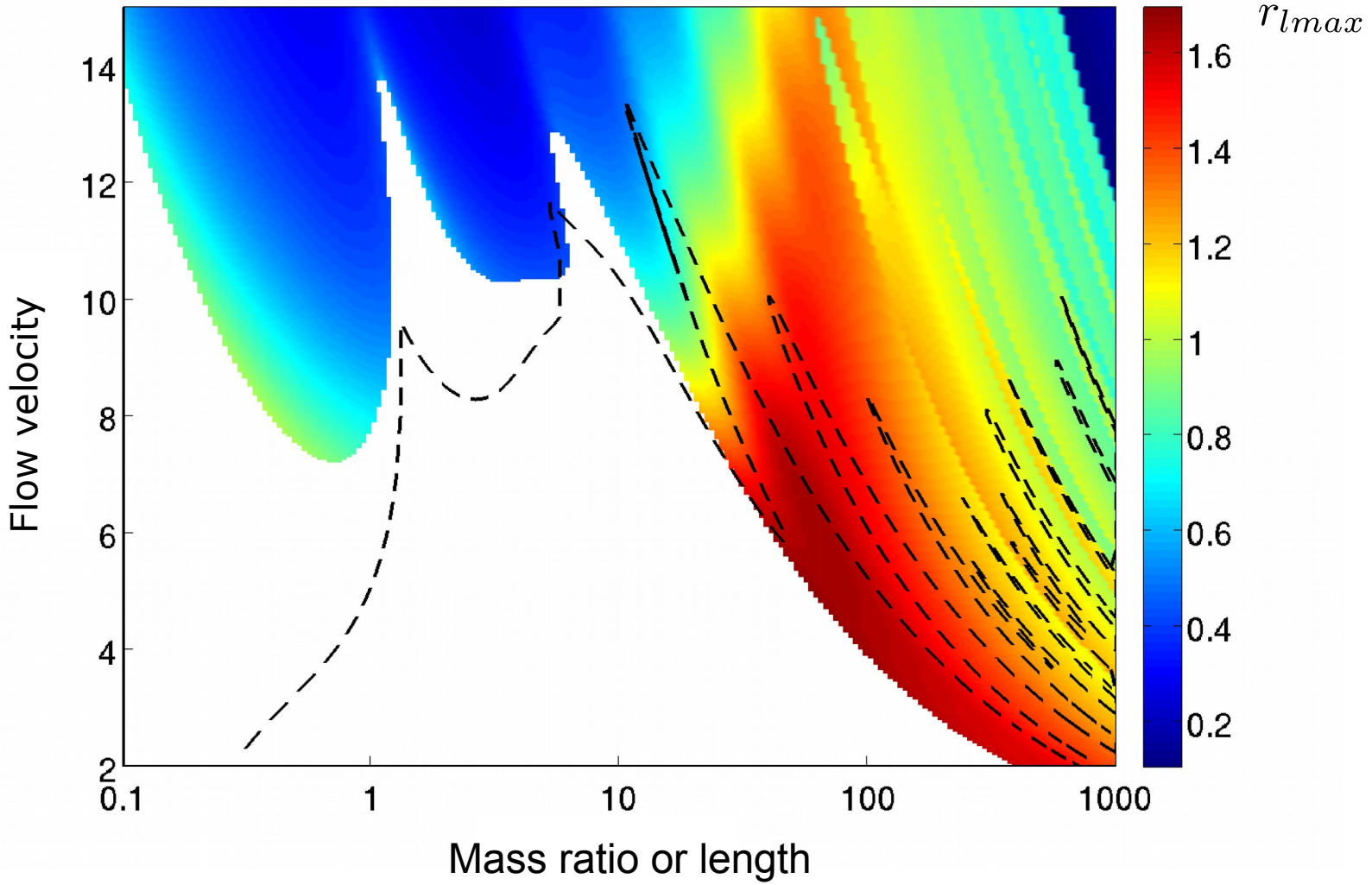


Efficiency is maximized when system is destabilized by piezoelectric coupling

# OUTLINE

**Flow energy harvesting with piezoelectric plates**

Flow energy harvesting

The piezoelectric flag

Linear stability and efficiency

Non linear vibrations and efficiency

Coupling with resonant circuits

Discrete distributions of electrodes

Conclusions

# Non linear analysis : discrete distribution

- Non linear slender body model (Lighthill 1971, Candelier et al 2011, Eloy et al 2012) coupled with a piezoelectric wave equation

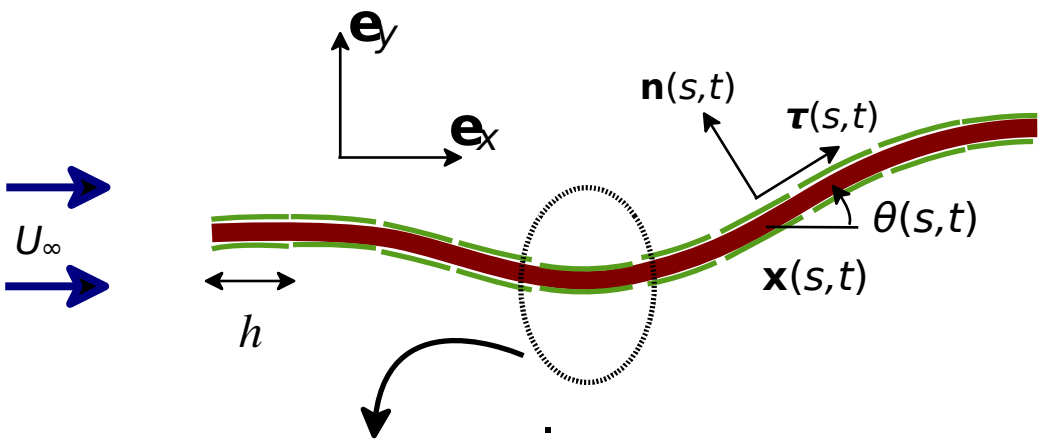


Inextensible Euler-Bernoulli beam :

$$\mu \frac{\partial^2 \underline{X}}{\partial T^2} = \frac{\partial}{\partial S}\left[F_t \underline{\tau} - \frac{\partial \mathcal{M}}{\partial S}\underline{n}\right] + \underline{F}_f$$

$$\frac{\partial \underline{X}}{\partial S} = \underline{\tau}$$

Piezoelectric coupling (discrete distribution) :

$$\bar{Q}_i = \bar{C}V_i + \chi[\theta]_{s_i^+}^{s_i^-} \quad i = 1..N$$

$$\mathcal{M} = B\frac{\partial \theta}{\partial S} - \sum_i^N \chi V_i F_i$$

$$F(Q_i, V_i) = 0 \quad i = 1..N$$

(+ clamped-free boundary conditions)

$$\underline{F}_f = \underline{F}_{\text{reactive}} + \underline{F}_{\text{resistive}}$$

$$= -m_a \rho_f H^2 \left(\frac{\partial U_n}{\partial T} - \frac{\partial U_n U_t}{\partial S} + \frac{1}{2}U_n^2 \frac{\partial \theta}{\partial S}\right)\underline{n} - \frac{1}{2}\rho_f H C_D U_n |U_n| \underline{n}$$

# Non linear analysis : continuous distribution

- Non linear slender body model (Lighthill 1971, Candelier et al 2011, Eloy et al 2012) coupled with a piezoelectric wave equation

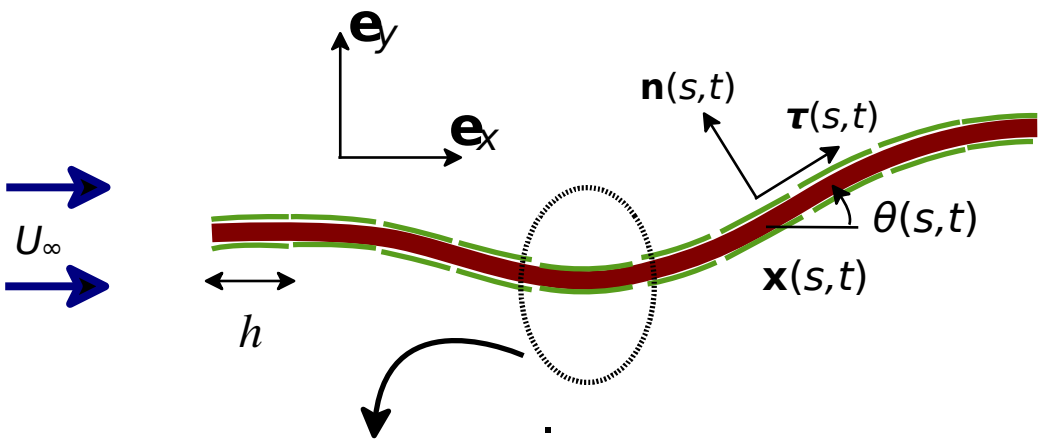


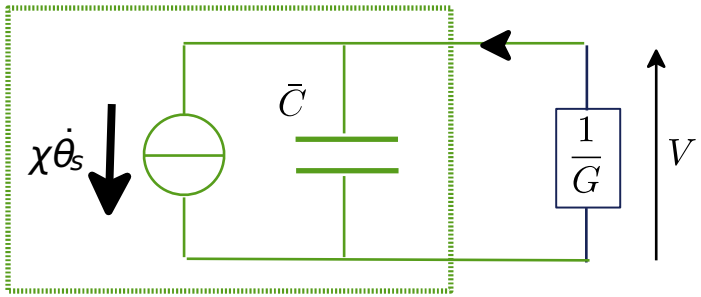


Inextensible Euler-Bernoulli beam :

$$\mu \frac{\partial^2 \underline{X}}{\partial T^2} = \frac{\partial}{\partial S}\left[F_t \underline{\tau} - \frac{\partial \mathcal{M}}{\partial S}\underline{n}\right] + \underline{F}_f$$

$$\frac{\partial \underline{X}}{\partial S} = \underline{\tau}$$

Piezoelectric coupling (continuous distribution) :

$$\bar{Q} = \bar{C}V + \chi \frac{\partial \theta}{\partial S}$$

$$\mathcal{M} = B\frac{\partial \theta}{\partial S} - \chi V$$

$$F(Q,V) = 0$$

(+ clamped-free boundary conditions)

$$\underline{F}_f = \underline{F}_{\text{reactive}} + \underline{F}_{\text{resistive}}$$

$$= -m_a \rho_f H^2 \left(\frac{\partial U_n}{\partial T} - \frac{\partial U_n U_t}{\partial S} + \frac{1}{2}U_n^2 \frac{\partial \theta}{\partial S}\right)\underline{n} - \frac{1}{2}\rho_f H C_D U_n |U_n| \underline{n}$$

# Numerical methods

- **Method 1** : Full non linear dyamics (used for the continuous problem)
  - Flag meshed using Chebyshev-Lobatto nodes
  - Chebyshev collocation method to compute spatial derivatives and integrals
  - The resulting nonlinear system is integrated in time solved using Broyden's method

- **Method 2** : Weakly non linear dynamics (used for the discrete problem)
  - Projection of dynamical equilibrium equation onto the $x$ and $y$ direction
    $\rightarrow$ two equations for $x(s,t)$ and $y(s,t)$
  - Horizontal projection used to eliminate the tension
  - x eliminated using the inextensibility condition
  - Terms up to $O(y^3)$ are kept
  - Expansion of $y$ on a few beam eigenmodes
  - Discrete set of coupled non linear oscillators
  - The resulting nonlinear system is integrated in time solved using Broyden's method

# Efficiency

- Windmill type efficiency :

$$\eta = \frac{\text{Power harvested in the electrial circuits}}{\text{Fluid's kinetic energy flux through the surface occupied by oscillations}} \propto \frac{A^2}{A}$$

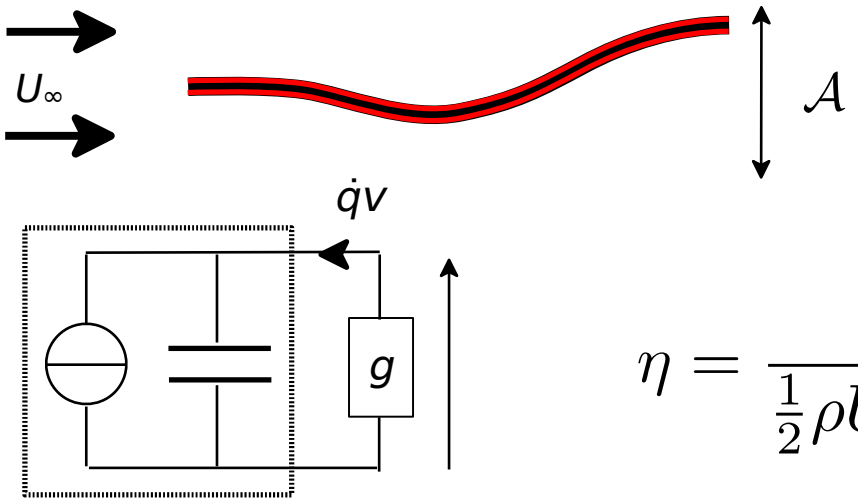


$$\eta = \frac{\mathcal{P}}{\frac{1}{2}\rho U_\infty^3 \mathcal{A}}$$

$$\mathcal{P}(t) = \int_0^L g v^2 ds \qquad \text{(continuous)}$$

$$\mathcal{P}(t) = \sum_i^N G V_i^2 \qquad \text{(discrete)}$$

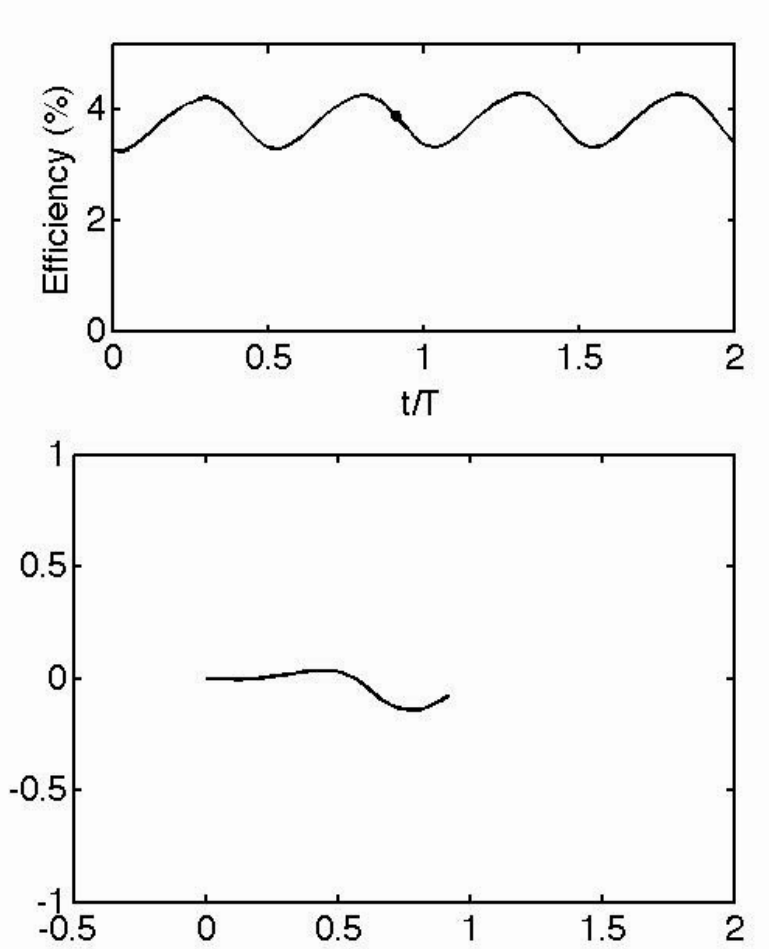

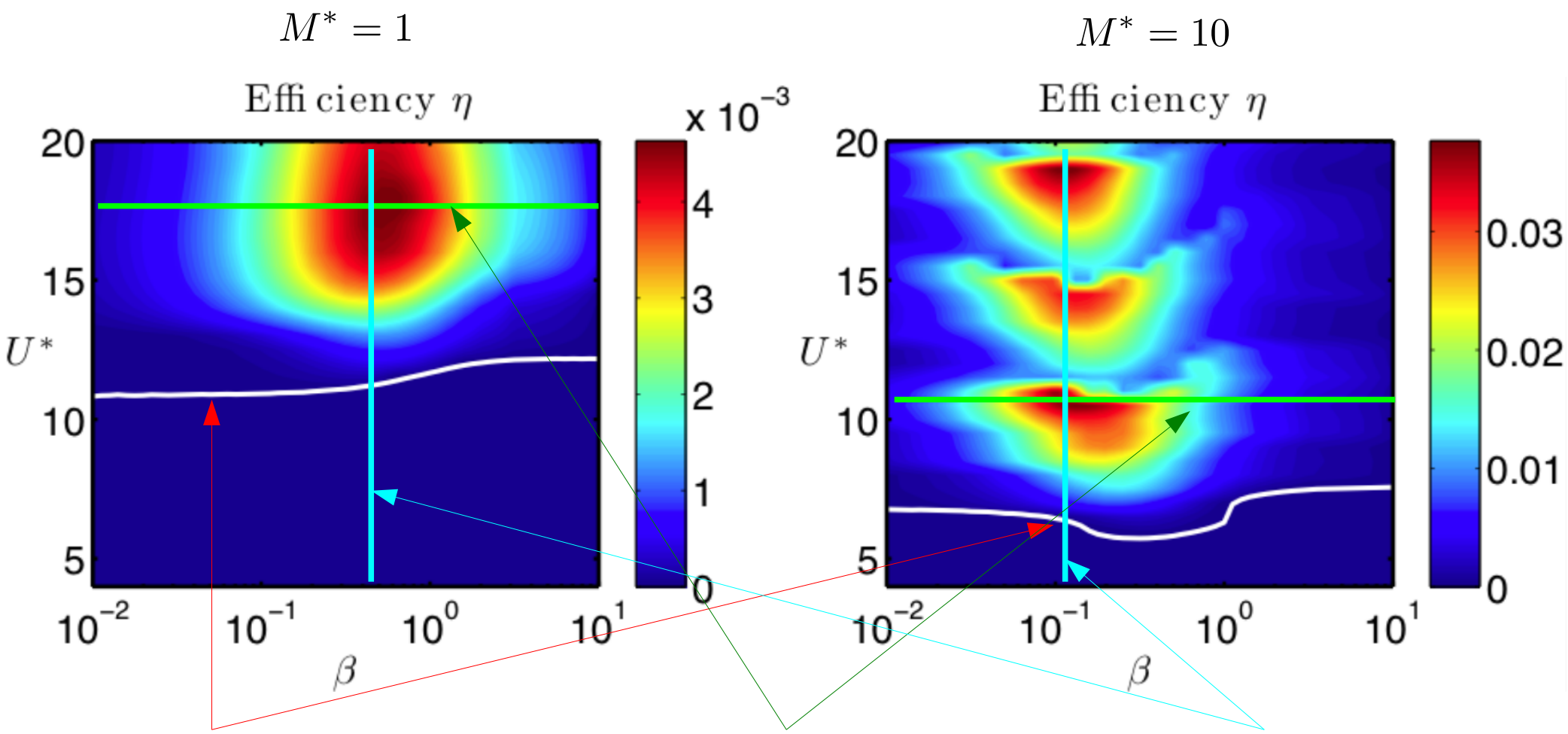


Linear stability treshold

Effect of the tuning ratio

Effect of the flow velocity

Destabilisation due to piezoelectric coupling at high M*

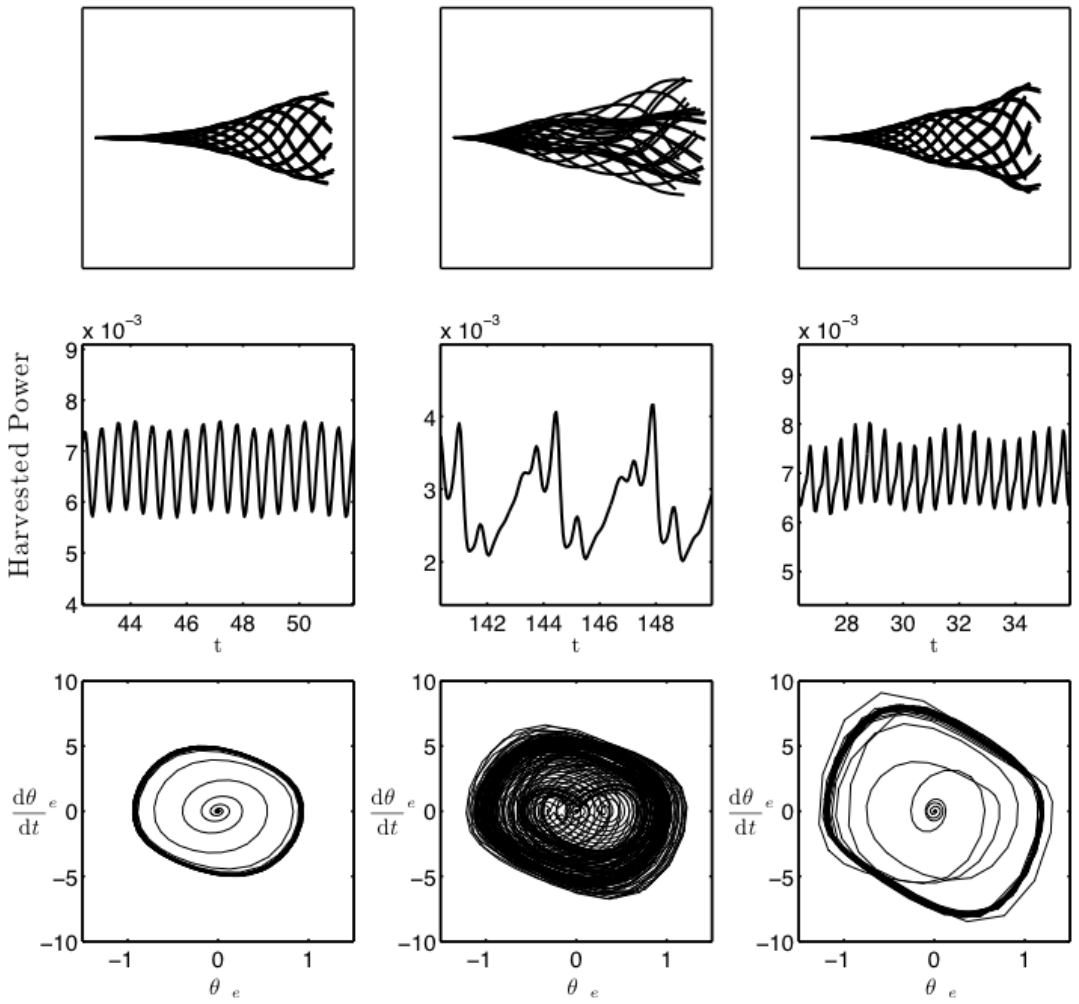


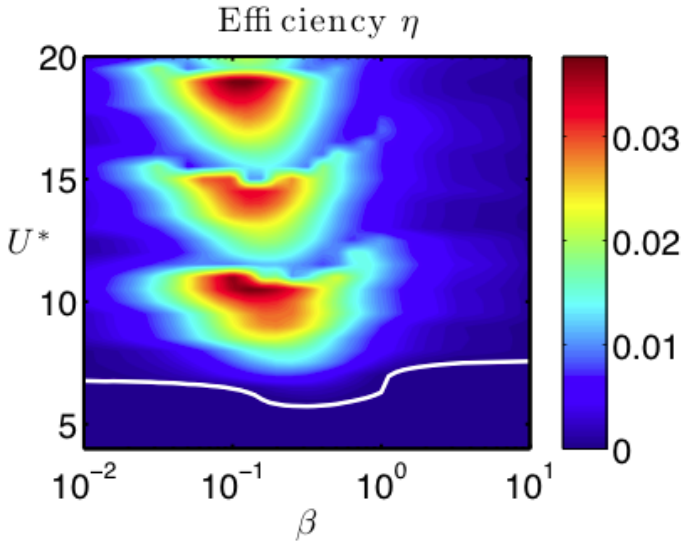


Mode switching events

# Non linear result

Efficiency for a perfect tuning of the output circuit

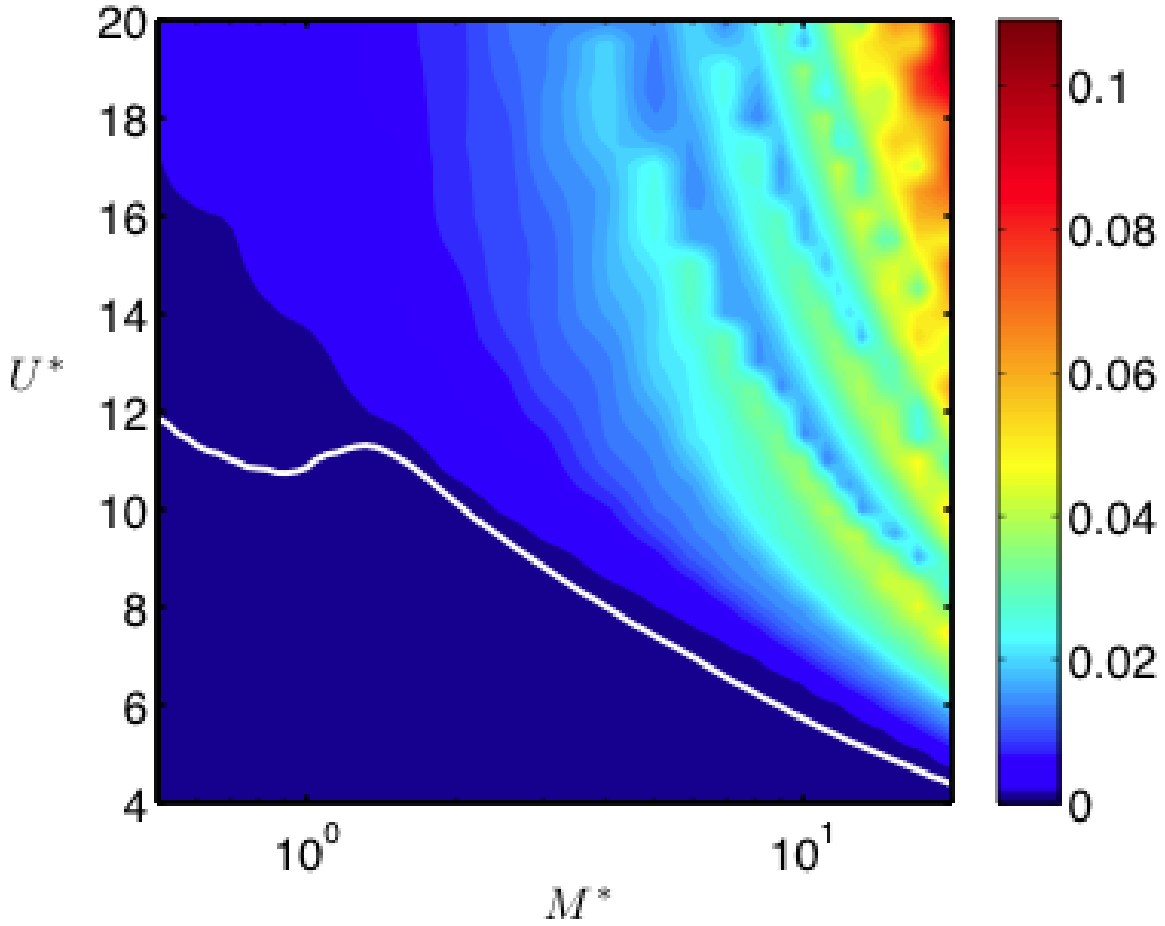


- Up to 10% of the incoming kinetic energy flux can be dissipated
- High efficiency regions are however associated with a higher sensitivity to the flow velocity

# OUTLINE

**Flow energy harvesting with piezoelectric plates**

Flow energy harvesting

The piezoelectric flag

Linear stability and efficiency

Non linear vibrations and efficiency

Coupling with resonant circuits

Discrete distributions of electrodes

Conclusions

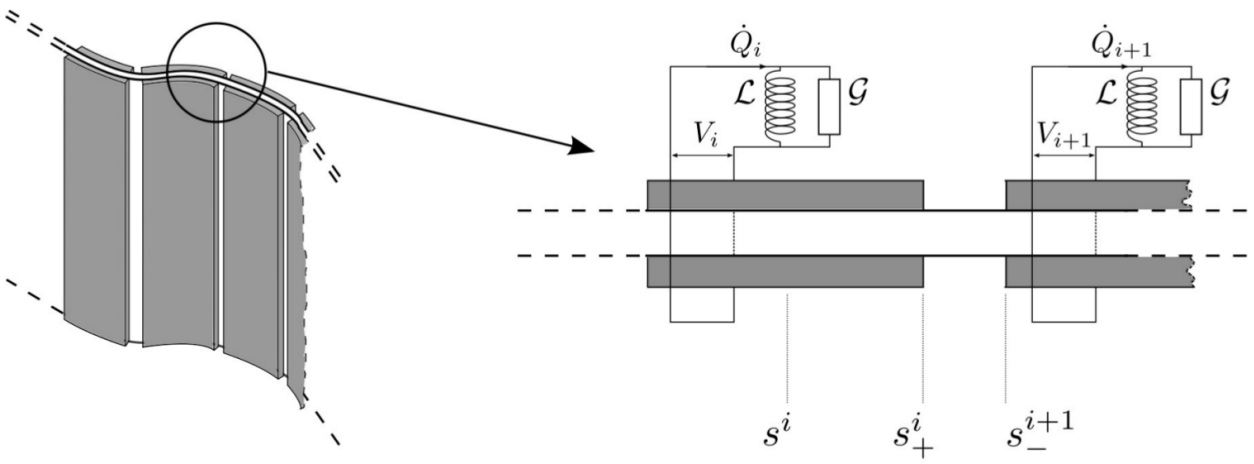


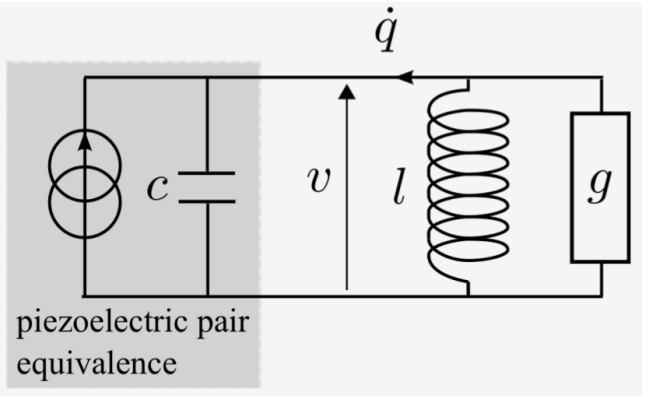


$$\frac{\partial^2 \mathbf{x}}{\partial t^2} = \frac{\partial}{\partial s}\left[T\boldsymbol{\tau} - \frac{\partial}{\partial s}\left(\frac{1}{U^{*2}}\frac{\partial \theta}{\partial s} - \frac{1}{U^*}\alpha v\right)\mathbf{n}\right] + M^*\mathbf{F}_{\text{fluid}},$$

$$\mathbf{F}_{\text{fluid}} = -m_a H^*\left[\frac{\partial U_n}{\partial t} - \frac{\partial U_n U_\tau}{\partial s} + \frac{1}{2}U_n^2\frac{\partial \theta}{\partial s}\right]\mathbf{n} - \frac{1}{2}C_d|U_n|U_n\mathbf{n},$$

$$\beta\omega_0^2 v + \frac{\partial v}{\partial t} + \beta\frac{\partial^2 v}{\partial t^2} + \frac{\alpha\beta}{U^*}\frac{\partial^3 \theta}{\partial t^2 \partial s} = 0,$$

**Parameters :** $M^* = \dfrac{\rho_f L}{\mu}, \quad U^* = UL\sqrt{\dfrac{\mu}{B}} = V^* M^*, \quad H^* = \dfrac{H}{L},$

$$\beta = \frac{cU_\infty}{gL} = \frac{\gamma}{M^*}, \quad \alpha = \frac{\chi}{\sqrt{cB}}, \quad \omega_0 = \frac{L}{U\sqrt{lc}}.$$

# Linear stability

$$M^* = 1, \quad H^* = 0.5, \quad \alpha = 0.3$$

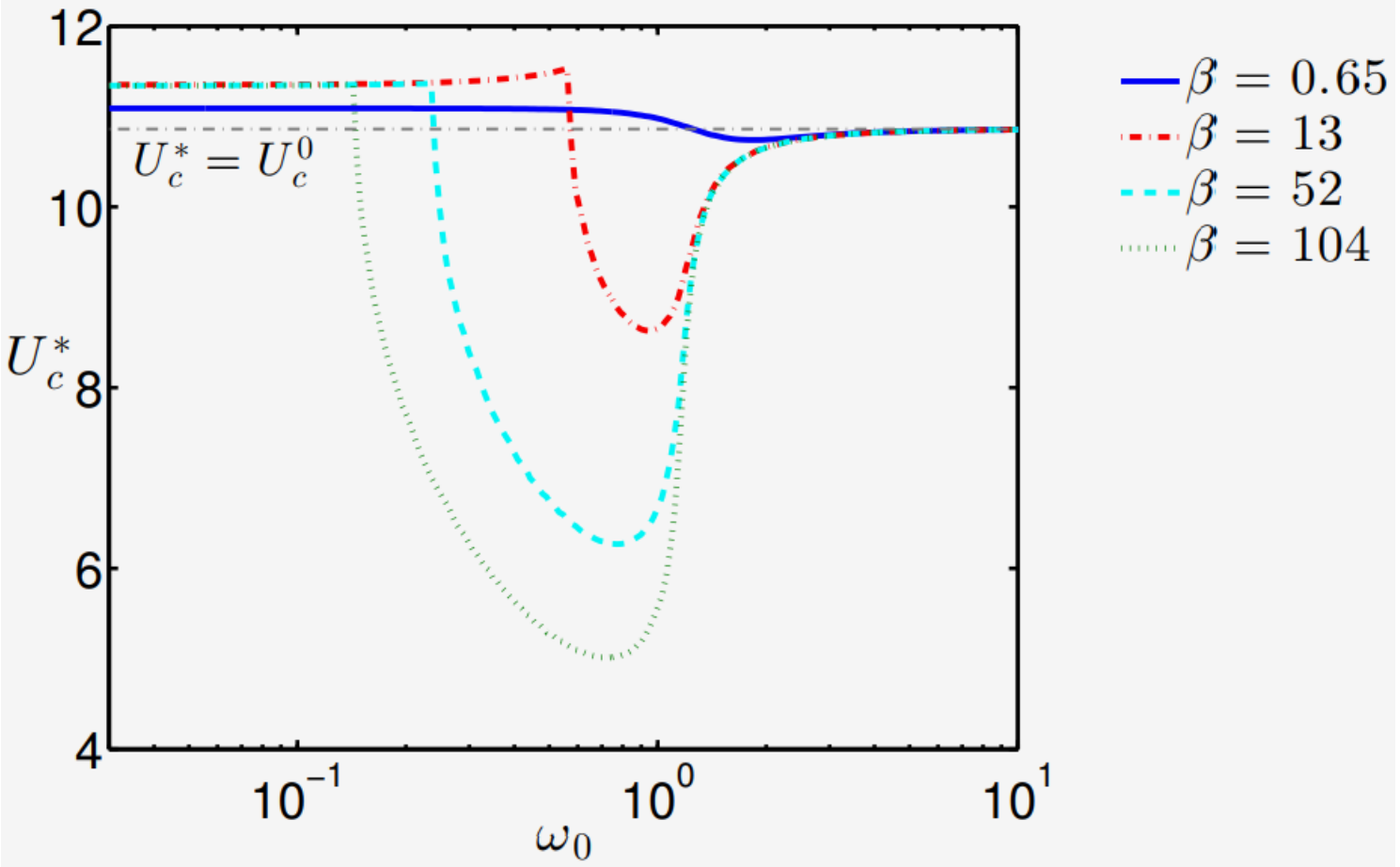


Destabilization induced by coupling with resonant circuits

# Nonlinear analysis : Lock-in

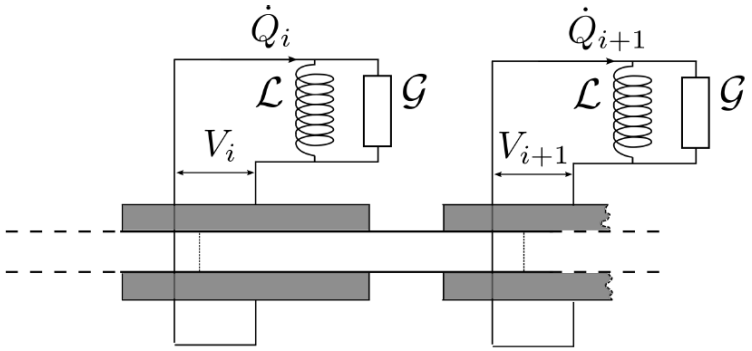


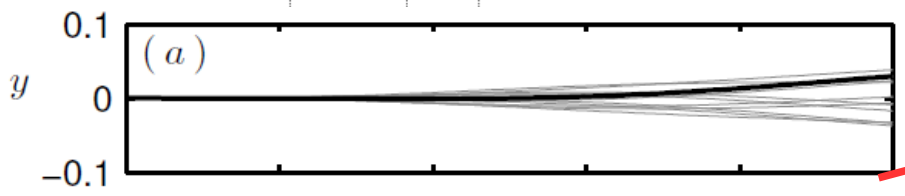


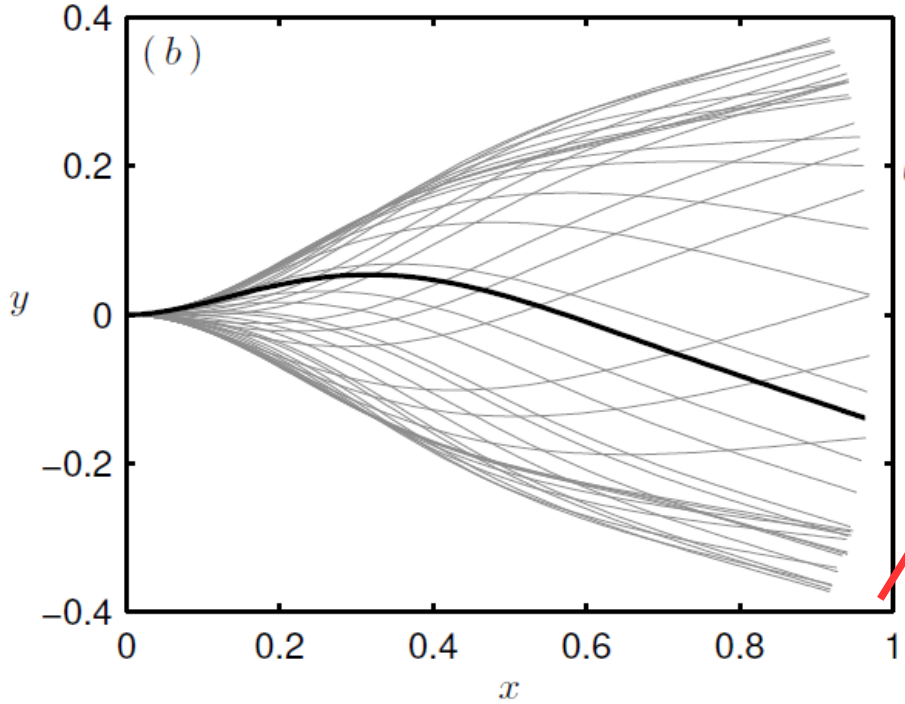


$M^* = 1, \quad U^* = 13, \quad H^* = 0.5, \quad \alpha = 0.3$

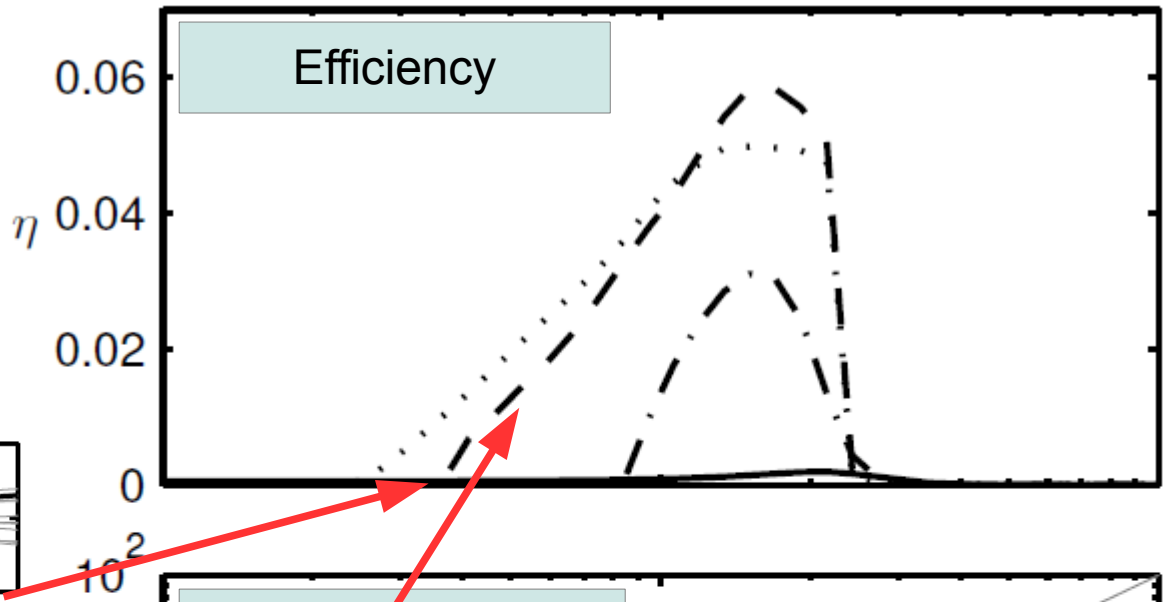


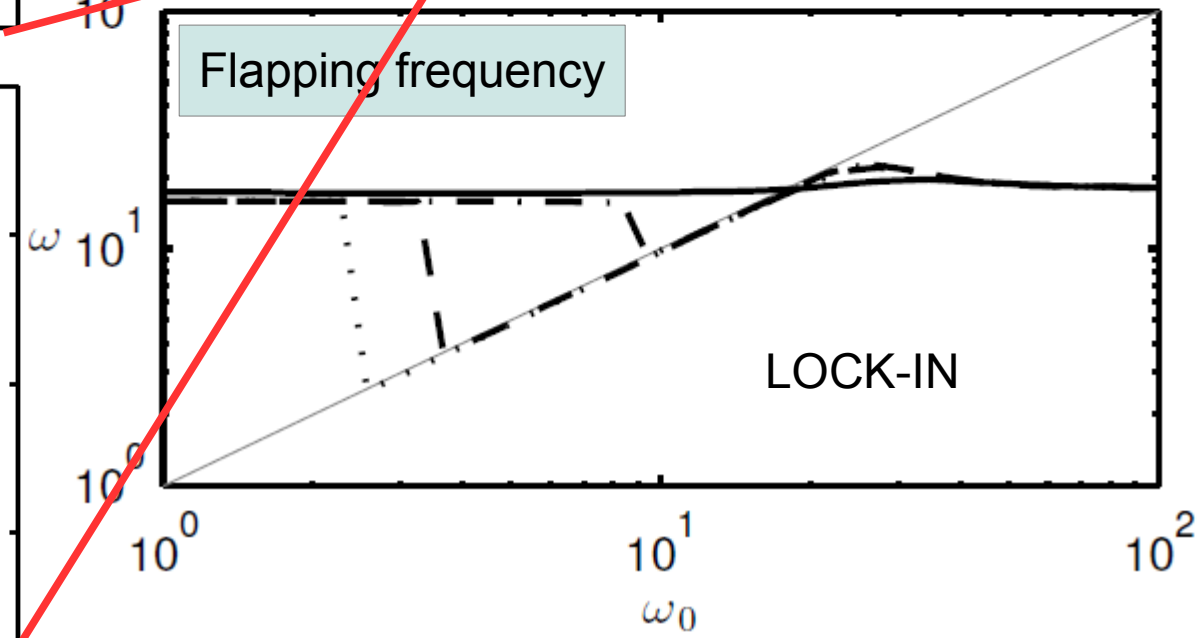


Circuit frequency

# Lock-in phenomenon in vortex-induced vibrations (VIV)

*Thiria & Cadot*

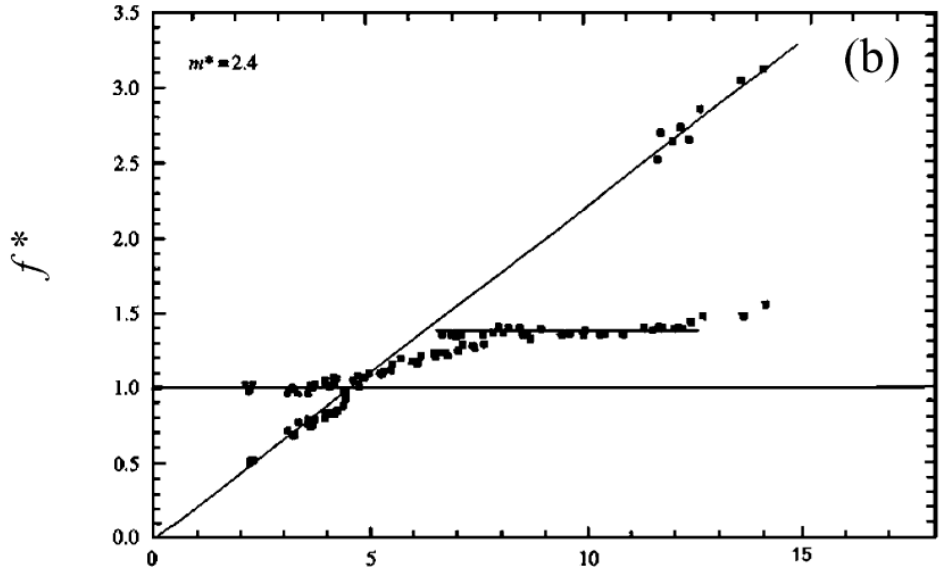


*Williamson & Govardhan, 2004*

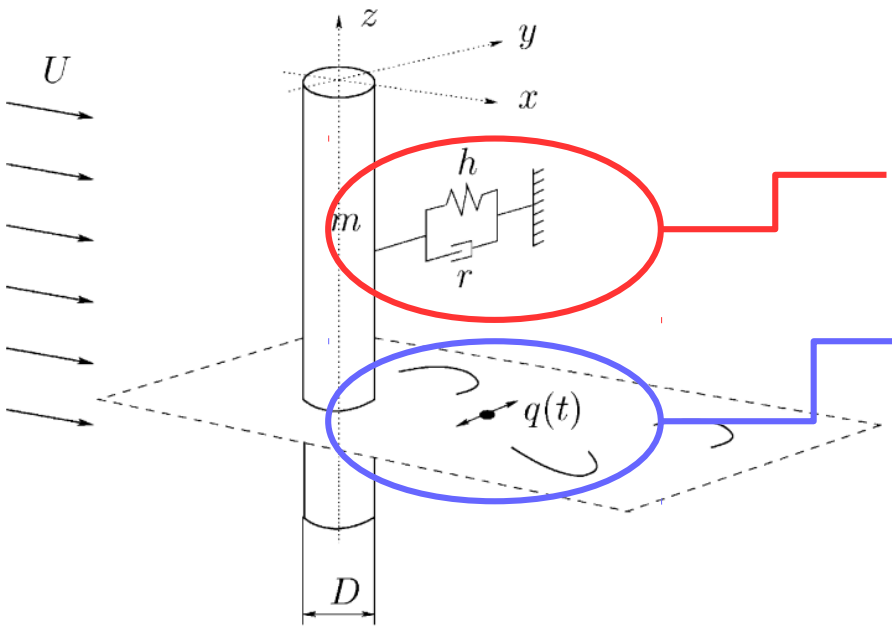


*Facchinetti et al, 2004*

Structural passive oscillator

Wake oscillator

# Experimental lock-in in the flag instability

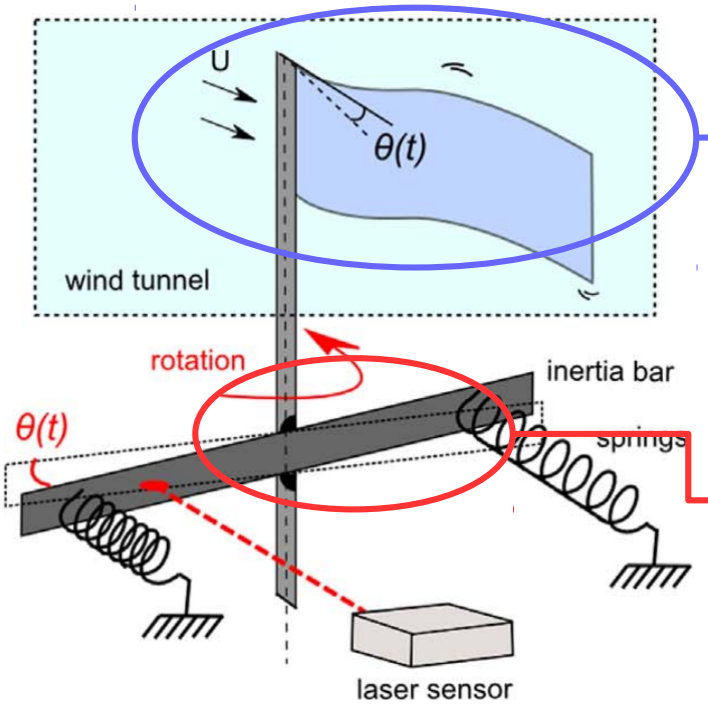


Active oscillator

Structural passive oscillator

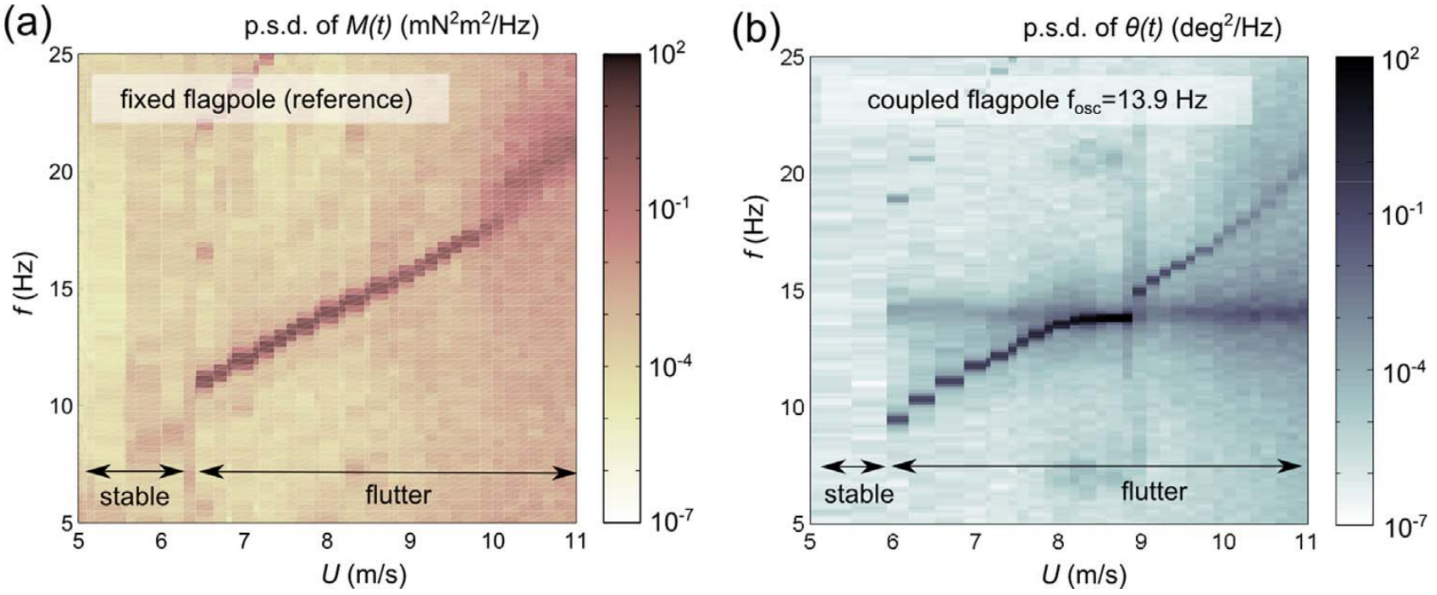


*Virot et al, 2016*

# Experiments

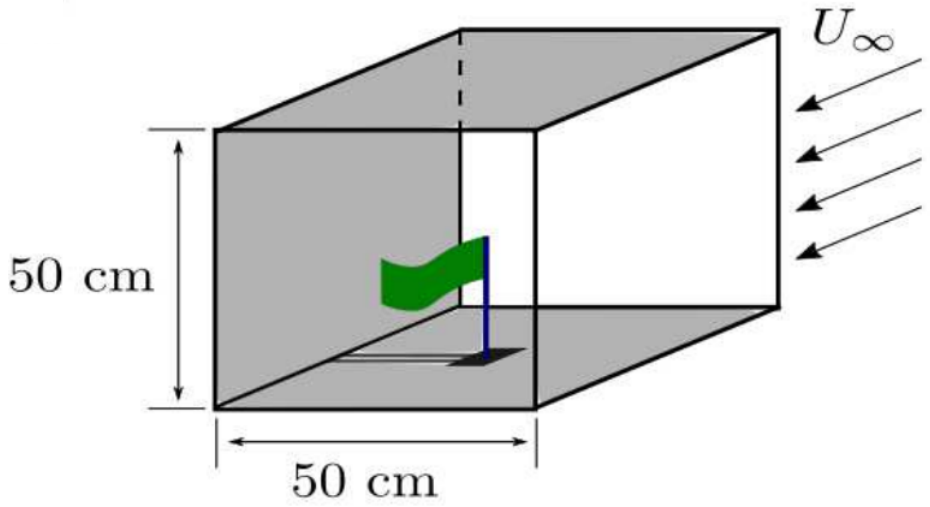


PVDF flag in a wind tunel

Flag covered by a unique piezoelectric pair

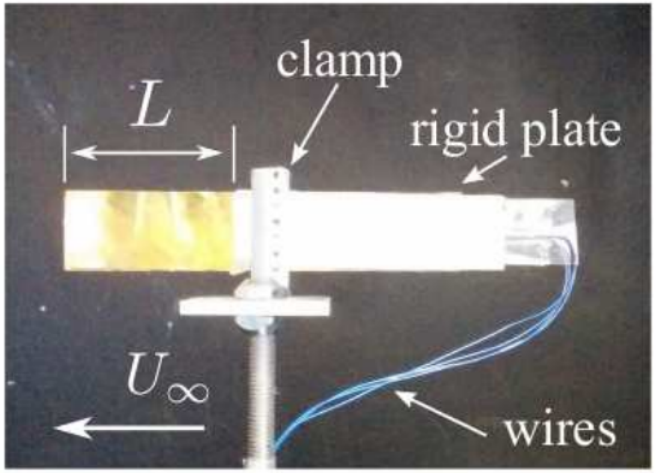


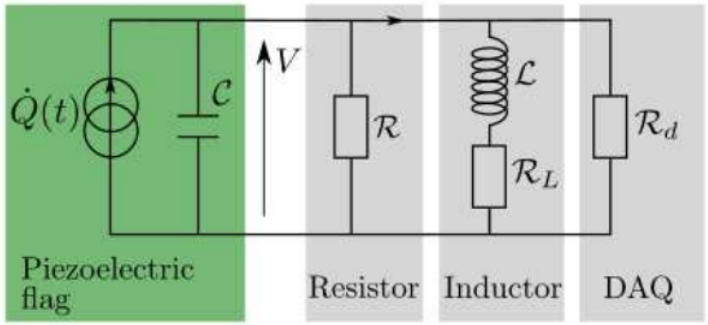

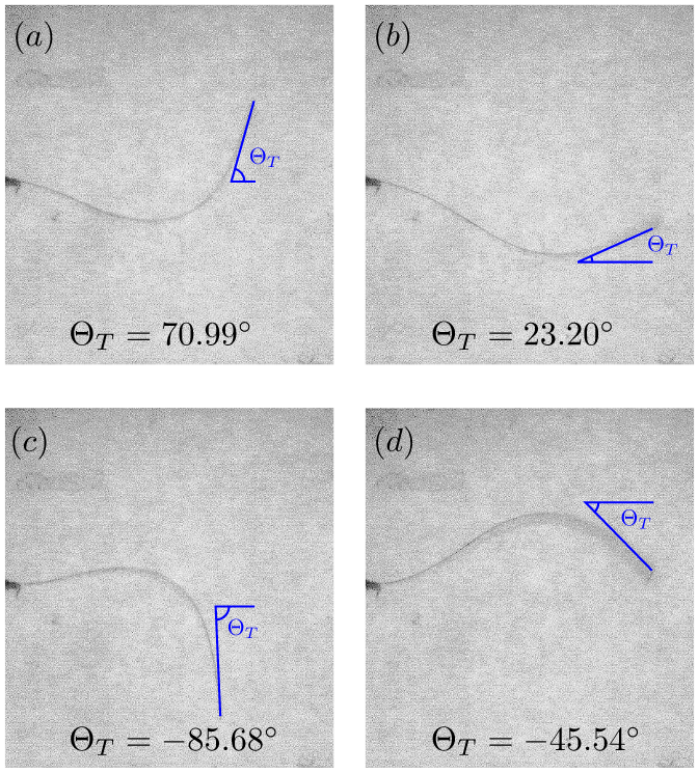


## Parameters estimation :

- Bending stiffness : free vibration frequency measurements
- Coupling coefficient $\chi$ : estimation from the free-end angle during vibration with a large impedance in place of the harvesting circuit

$$R\chi\dot{\theta_T} + RC\dot{V} + V = 0$$

Assuming harmonic signals :

$$V = V_0 e^{i2\pi ft} \qquad \theta_T = \theta_0 e^{i(2\pi ft+\varphi)}$$

$$\chi = \frac{V_0}{2\pi f\theta_0}\sqrt{\frac{1}{R^2} + 4\pi^2 f^2 C^2}$$

| | $L$ (cm) | $U_\infty$ (m/s) | $f$ (Hz) | $\mathcal{L}$ (H) | $\alpha$ | $M^*$ | $H^*$ | $U^*$ | $\omega_0$ |
|---|---|---|---|---|---|---|---|---|---|
| Case A | 6 | 20.9 | 56.8 | 530 | 0.085 | 0.410 | 0.417 | 17.91 | 1.06 |
| Case B | 8 | 17.8 | 41.0 | 1000 | 0.1 | 0.547 | 0.313 | 21.18 | 1.14 |

# Improvement by resonance

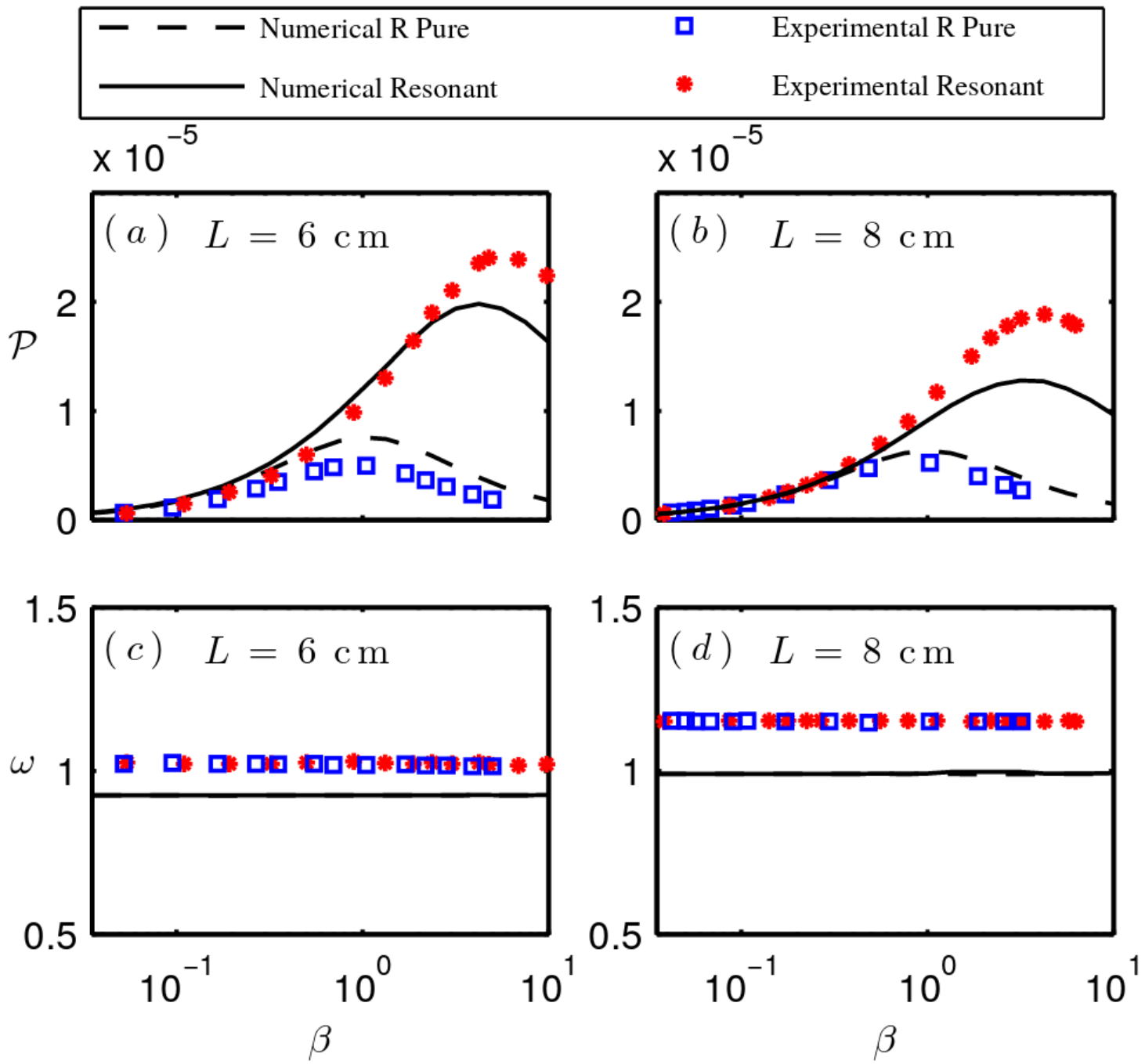


LOCK-IN ?

## Numerical results

$$\alpha = 0.3 \quad \beta = (13, 52)$$

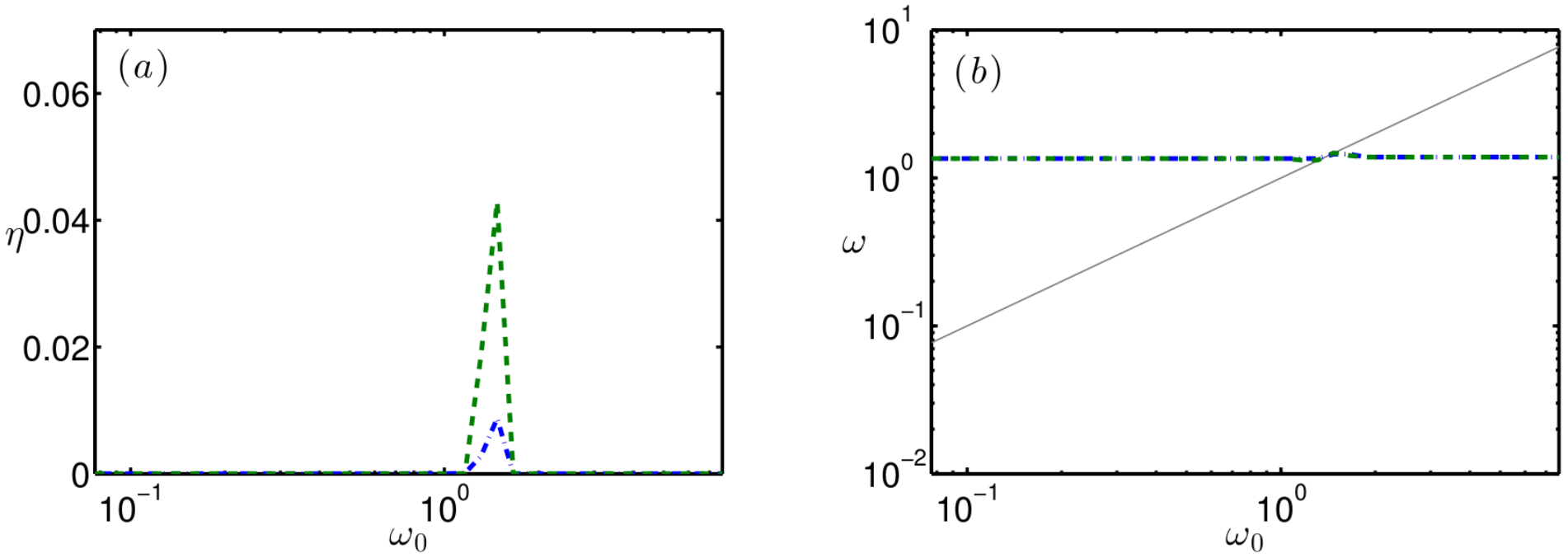


Lock-in can be observed for a single electrode coverage, but for large values of the coupling coefficient and in a narrow frequency band.

# OUTLINE

**Flow energy harvesting with piezoelectric plates**

Flow energy harvesting

The piezoelectric flag

Linear stability and efficiency

Non linear vibrations and efficiency

Coupling with resonant circuits

Discrete distributions of electrodes

Conclusions

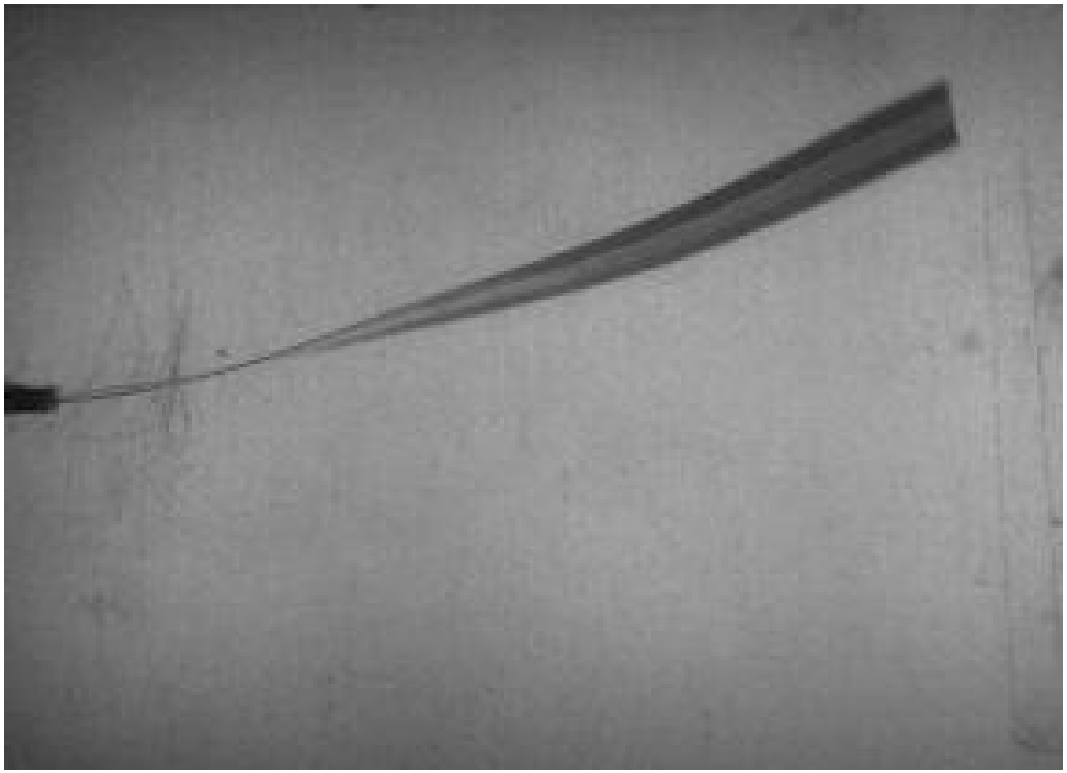

# Influence of the electrode positioning

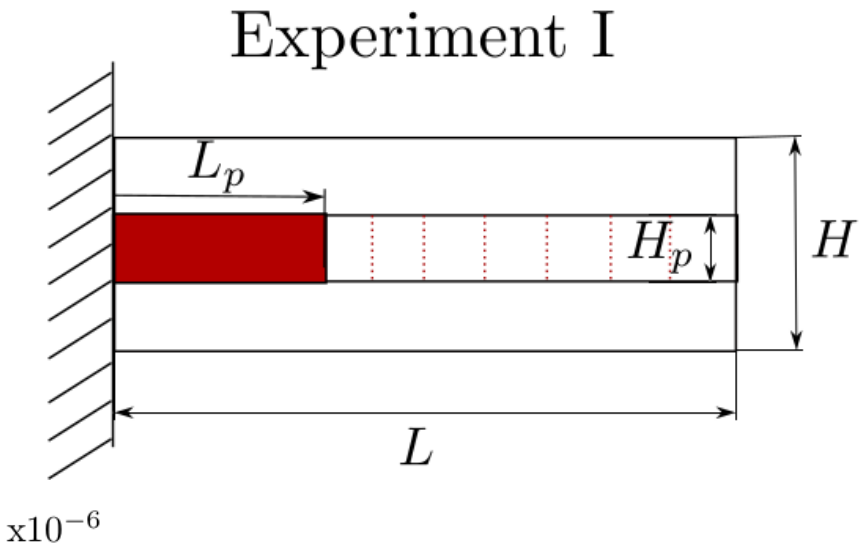


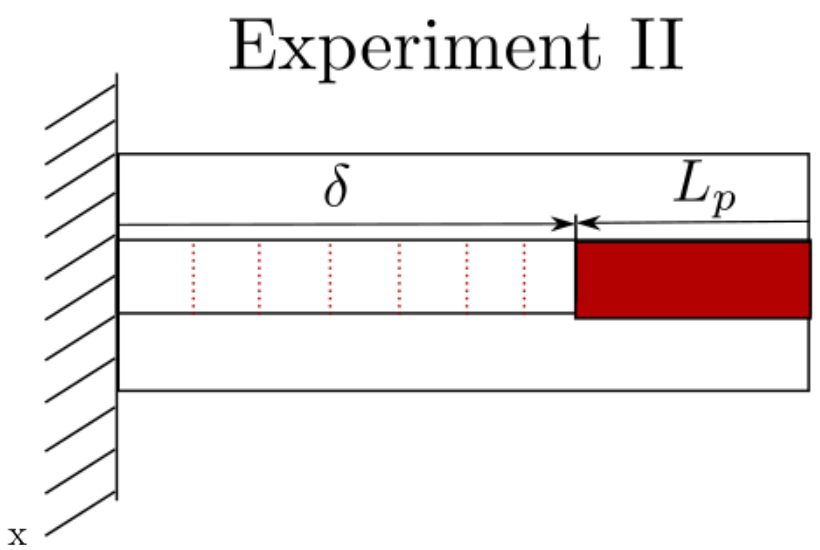


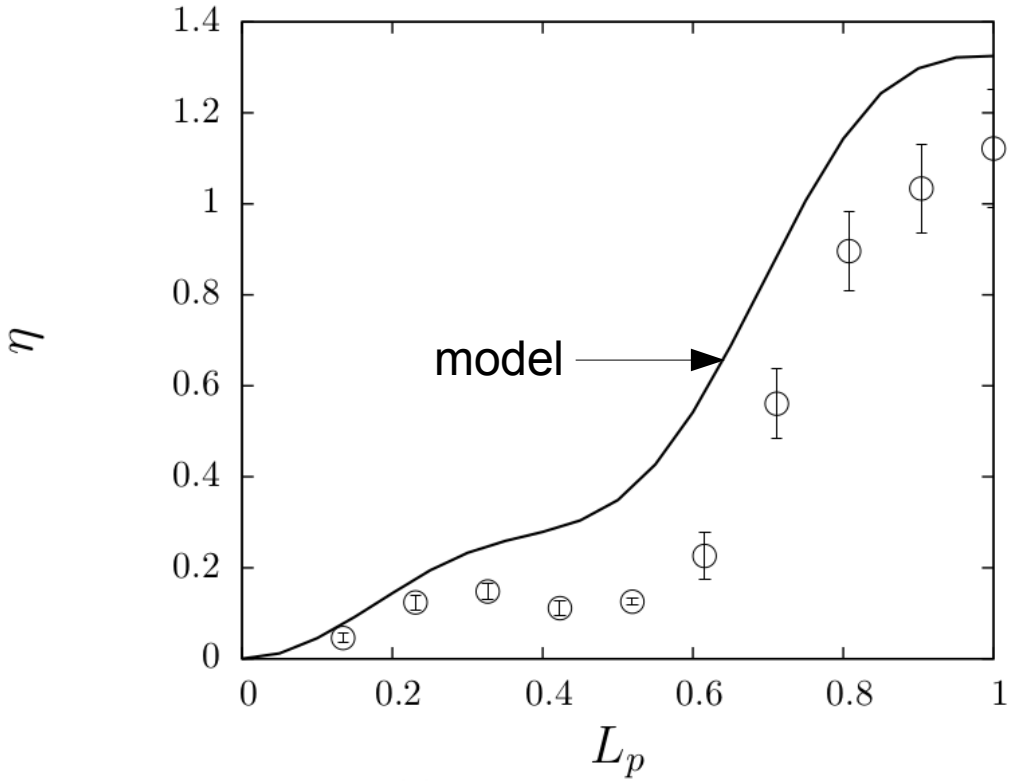


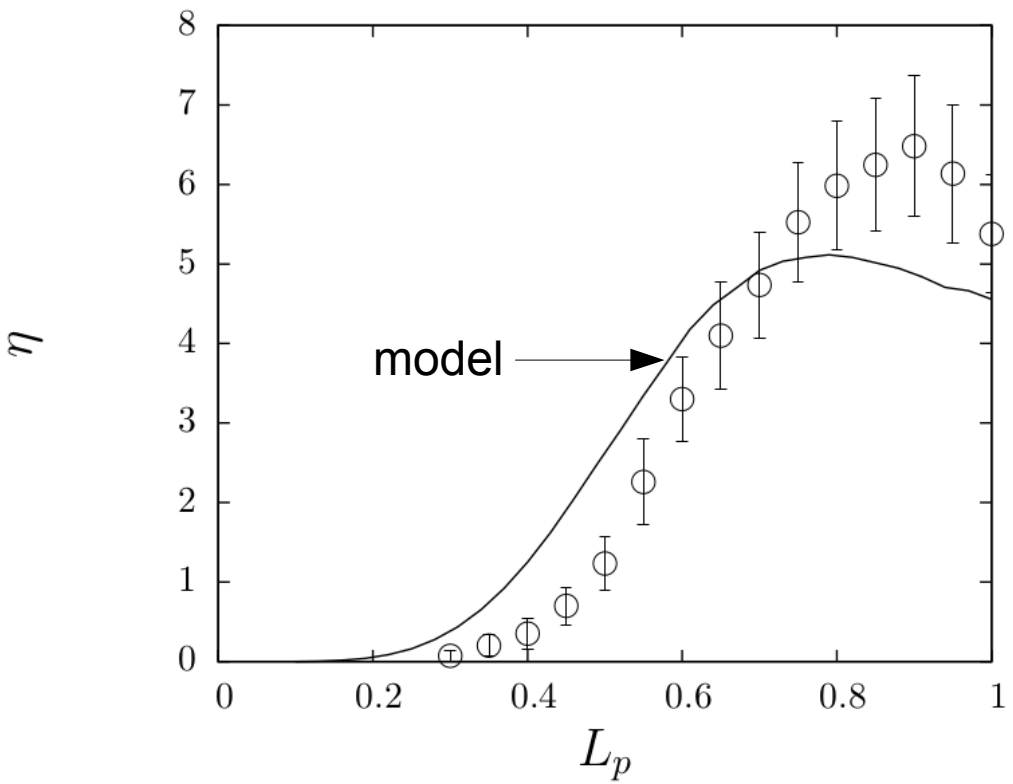

# Number of piezoelectric patches Np

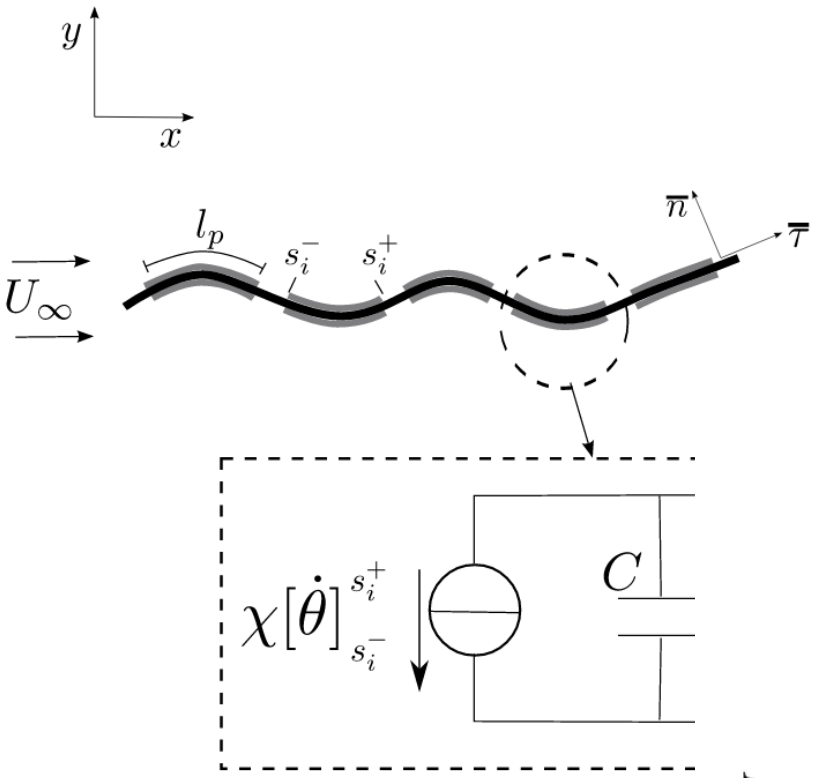


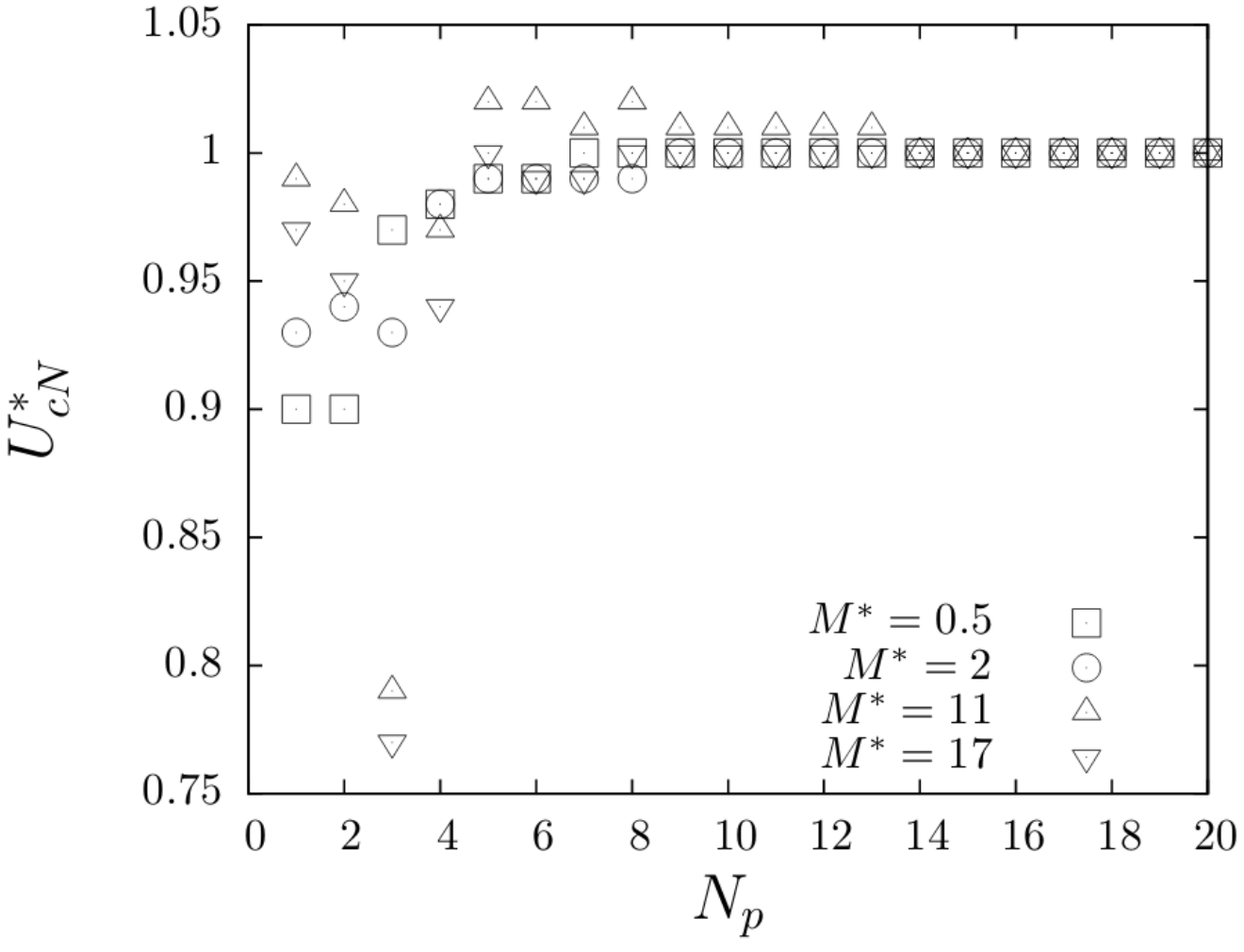

# Finite length piezoelectric patches (Piñeirua et al 2015)

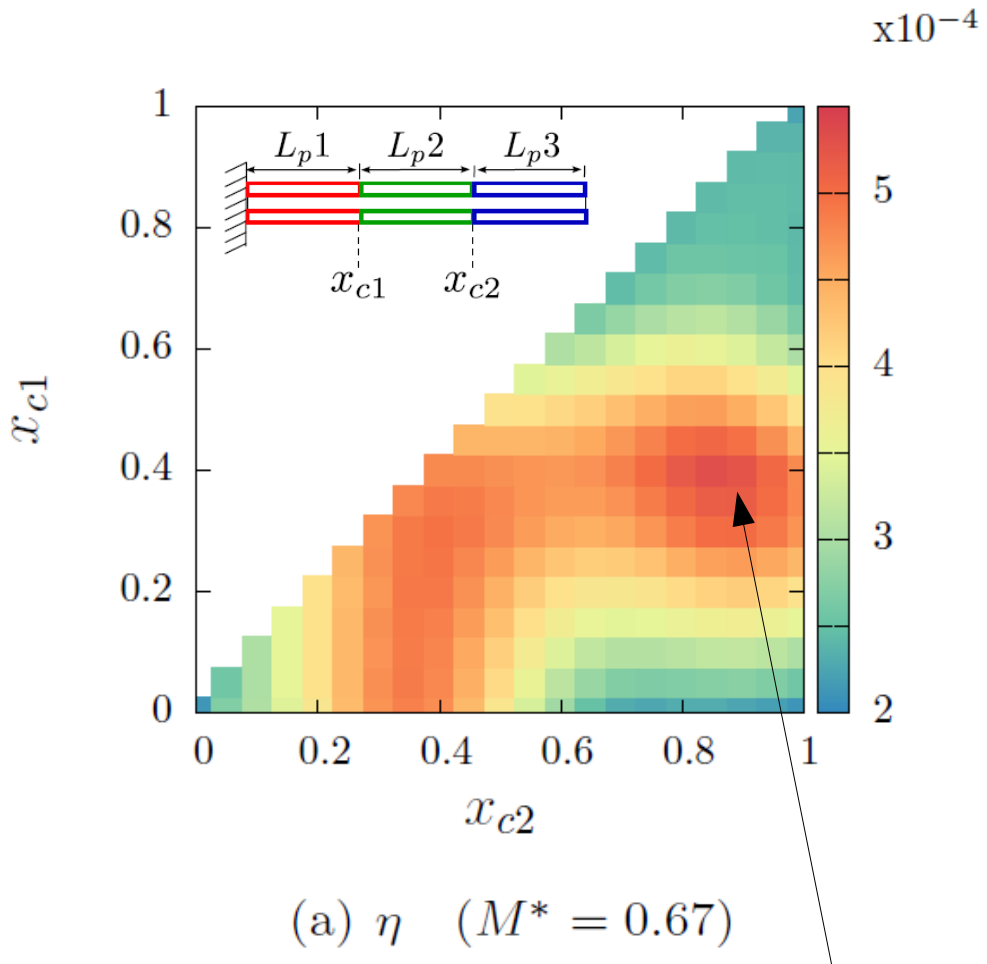


(a) $\eta \quad (M^* = 0.67)$

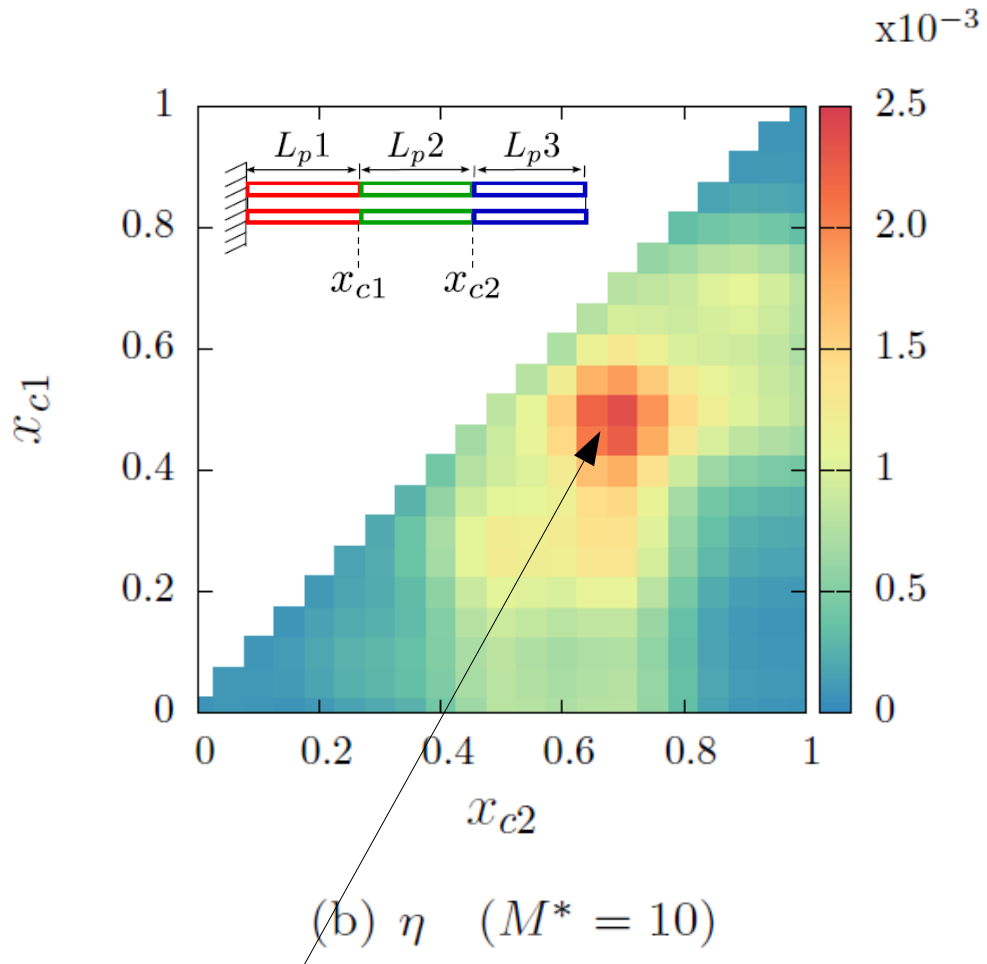


(b) $\eta \quad (M^* = 10)$

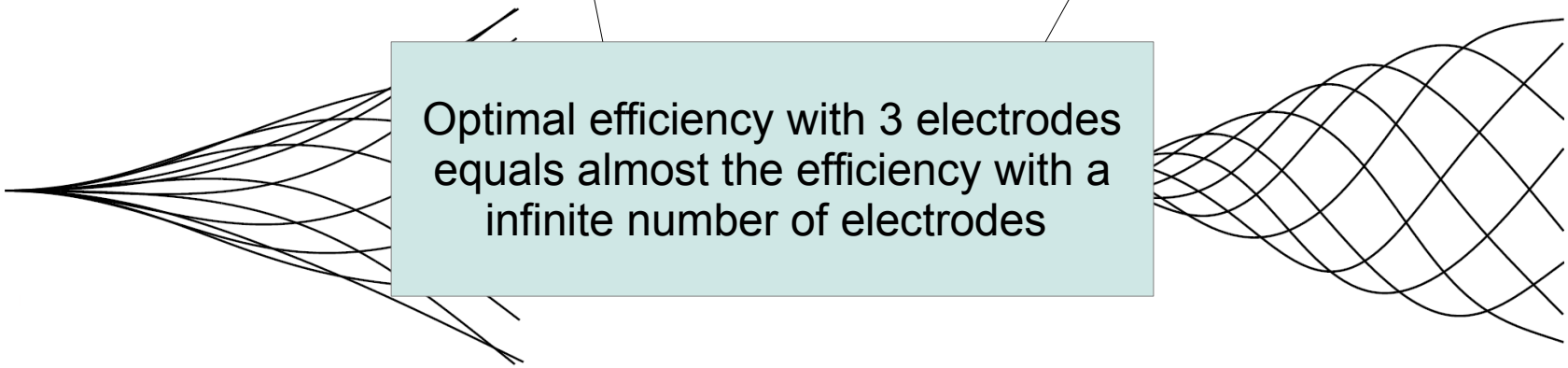

Optimal efficiency with 3 electrodes equals almost the efficiency with a infinite number of electrodes

# OUTLINE

**Flow energy harvesting with piezoelectric plates**

Flow energy harvesting

The piezoelectric flag

Linear stability and efficiency

Non linear vibrations and efficiency

Coupling with resonant circuits

Discrete distributions of electrodes

Conclusions

# Main results

- Linear
  - Linear stability analysis in the infinite and finite cases
  - NEW → destabilization by piezoelectric coupling
  - Negative energy waves maximize efficiency
  - Importance of the tuning of the fluid-solid and electric frequencies
  - Efficiency scales as $\alpha^2$
- Non linear
  - A significant fraction of the kinetic energy flux can be harvested (~10%)
  - Importance of the tuning of the fluid-solid and electric frequencies
  - High mass ratio (or long systems) tends to improve efficiency
  - High sensitivity to the flow velocity in the high-efficiency regimes.
  - Eelctric resonance or lock-in can significantly improve efficiency
  - Discrete distribution of electrodes : a few electrodes can achieve the same efficiency as a continuous distribution


Doaré, O. & Michelin, S. (2011), Piezoelectric coupling in energy-harvesting fluttering flexible plates : linear stability analysis and conversion efficiency. Journal of Fluids and Structures, 27(8) :1357–1375.

Michelin, S. & Doaré, O. (2013), Energy harvesting efficiency of piezoelectric flags in axial flows. Journal of Fluid Mechanics, 714, 489-504.

Xia, Y., Michelin, S., Doaré, O. (2015), Fluid-solid-electric lock-in of energy-harvesting piezoelectric flags, Physical Review Applied, 3, 014009.

Xia, Y., Doaré, O., Michelin, S. (2015), Resonance-induced enhancement of flow energy harvesters based on piezoelectric flags, Applied Physics Letters, 107(26), 263901.

Pineirua, M., Doaré, O., Michelin, S. (2015), Influence and optimization of the electrodes position in a piezoelectric energy harvesting flag, Journal of Sound and Vibration, 346, 2015, 200-215.

Xia, Y., Doaré, O., Michelin, S. (2016), Electro-hydrodynamic synchronization of piezoelectric flags, Journal of Fluids and Structures, 65, 398-410.

Pineirua, M., Michelin, S., Vasic, D. and Doaré, O. (2016), Synchronized switch harvesting applied to piezoelectric flags, Smart Materials and Structures, 25, 085004.